ChemComm

Accepted Manuscript

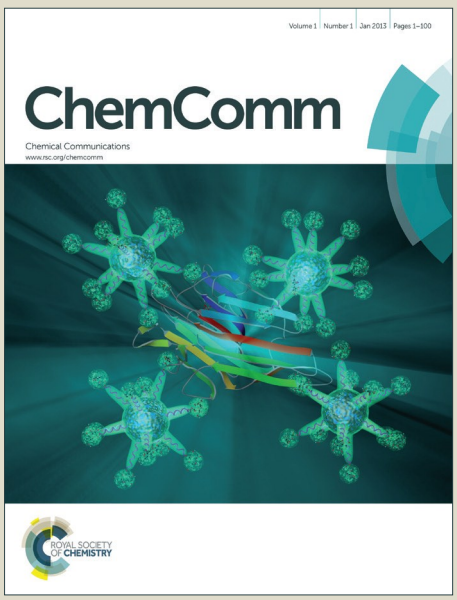

ROYAL SOCIETY OF CHEMISTRY

www.rsc.org/chemcomm

Chem Comm ChemComm Dynamic Article Links ►

Cite this: DOI: 10.1039/c0xx00000x

www.rsc.org/xxxxxx

FEATURE ARTICLE

Fused polycyclic aromatics incorporating boron in the core: Fundamentals and Applications†

Aude Escande[a] and Michael J. Ingleson*[a]

Received (in XXX, XXX) Xth XXXXXXXXX 20XX, Accepted Xth XXXXXXXXX 20XX
DOI: 10.1039/b000000x

The incorporation of boron into the core structure of fused polycyclic aromatics generates compounds with highly attractive properties that have recently received significant attention. Embedding boron into the backbone of ladder or 2D poly aromatic hydrocarbons is an underexplored approach to modulate optoelectronic properties, with tricoordinate boron representing a novel acceptor moiety for organic optoelectronic applications. Furthermore, the incorporation of boron into polycyclics containing other heteroatoms (e.g., chalcogens or pnictogens) leads to more extensive structural diversity and considerable ability to modify the frontier orbital energies and character, often in a controlled manner, to fine tune material properties for specific applications. This feature article summarizes the recent key developments in this field.

Introduction

Fused π conjugated systems, where neighbouring aromatic units are locked co-planar, are an attractive class of materials that have found widespread applications in organic field effect transistors, organic light emitting diodes and organic photovoltaics.[1] The incorporation of a range of main group elements into conjugated ladder molecules is a well-established method used to enhance optoelectronic properties e.g., by fine tuning frontier orbital energies. However, embedding boron atoms into fused structures is a relatively underexplored field. This in part is due to the synthetic challenges involved which has restricted the development of these compounds, particularly when compared to boron containing conjugated systems where boron is not embedded in the fused structure.[2] Successful incorporation of boron into fused conjugated materials introduces a formally vacant p orbital, provided boron remains three coordinate. The overlap between the empty p orbital on the electron deficient boron centre and the extended π system modulates key properties, including red shifting absorption and emission and enhancing charge mobility. Materials containing three-coordinate boron are therefore distinct to tetra-coordinate boron containing fused systems, which have been recently reviewed.[3]

Over the past decade structure property relationship studies indicate a distinction between C_3B (boron bound to three carbon atoms in the acene) containing fused structures and analogues containing heteroatom-boron bonds. The latter generally involve NR_2 or OR groups bonded to boron, with both being good π donors (relative to aromatic moieties) and thus Lewis acidity at boron in these fused structures is modulated with a concomitant effect on associated properties.[4] Compounds containing B-N bonds are thus omitted herein and have been recently reviewed elsewhere.[5] The considerable interest in the chemistry of boron containing fused materials with boron located in the annulated core combined with their significant potential prompts us to review the recent highlights in this exciting field, which covers contributions published up to the end of 2014.

Fundamental aspects of fused organo-boranes

Fused polyaromatic structures containing boron are most amenable to classification by the nature of the boracycle, i.e. five, six or seven membered and with or without additional heteroatoms. This review is therefore subdivided using this approach, though commonalities exist across each sub class.

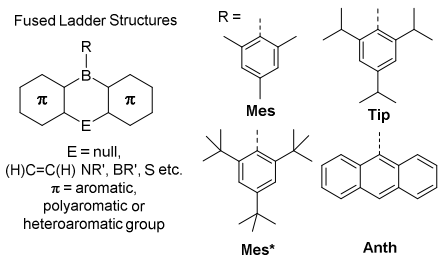

Scheme 1

The majority of the fused structures discussed herein can be classed as 'ladder' structures (Scheme 1, left), therefore contain one exocyclic substituent on boron. Preventing coordination of a fourth molecule to the Lewis acidic boron centre in these ladder structures is essential to maintain the desired electronic properties and provide stability to protic species that would otherwise lead

to protodeboronation. To provide sufficient kinetic stabilisation whilst minimising π donation to boron the boron centre is generally protected by a bulky aromatic exocyclic substituent. The most common group used for this purpose is the mesityl (Mes) group however, fused compounds containing only one mesityl substituent on boron have been found to be unstable to protic species, e.g., H_2O, in a number of cases. Boron substituents that are sterically more demanding than Mes have been successfully applied to enhance stability and other common examples are shown in Scheme 1. Due to their considerable steric bulk, these groups are invariably orientated perpendicular to the plane of the boracycle. These large exocyclic groups significantly reduce Lewis acidity at boron by effectively screening the formally vacant boron based orbital providing kinetic stability to H_2O and even enabling purification by column chromatography. Whilst the orthogonal arrangement minimises π delocalisation from the exocyclic substituent to boron these large substituents can preclude close intermolecular π-π interactions that are desirable for high charge mobility.

Fused structures containing borole moieties

Boroles are five-membered unsaturated boracycles that are antiaromatic possessing 4 π electrons. Whilst Eisch and co-workers pioneered these compounds in the 1960s,[6] recent years has seen significant fundamental and applied reactivity studies on borole containing compounds principally due to their high electrophilicity. Boroles have been the subject of reviews by Marder *et al.,*[7] which covered examples up to 2009, and by Braunschweig *et al.*, who presented an overview of non-fused boroles up to 2013.[8] This section therefore focuses on publications since 2008 where boroles have been incorporated into larger fused π systems. Earlier examples are included where appropriate for comparative purposes.

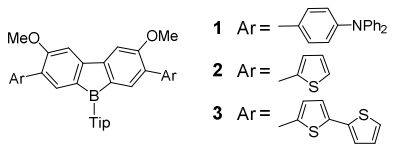

In early work Yamaguchi *et al.*[9] synthesised a number of dibenzoboroles substituted with thiophene or phenylamine groups, **1 - 3**. The π-extended boroles were synthesised from the appropriate 2,2'-diiodo-4,4'-dibromobiphenyl, with the two iodides used for formation of the central borole ring *via* lithiation and reaction with $TipB(OMe)_2$. The two bromo groups then allow for the extension of the conjugated system by Stille cross coupling. The photophysical studies of **1**, **2** and **3** show that all three compounds possess a large red-shift (97-100 nm) in THF relative to the related borole without an elongated π-system, suggesting extended π-conjugation along the carbon skeleton. Compounds **1 - 3** also displayed significant solvatochromism, for example, the fluorescence is 20 to 30 times less efficient in THF than in DMF. Yamaguchi *et al.* proposed that the solvatochromism is due to the coordination of the stronger donor solvent DMF to the boron atom, which was supported by the binding of fluoride from nBu_4NF (TBAF) in THF which led to similar photophysical properties to that observed in DMF.

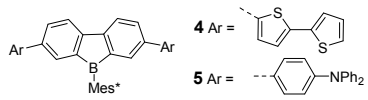

A subsequent study examined related compounds with Mes* substituents on boron in place of Tip.[10] In this case the Mes* substituted 4,4'-dihalo-dibenzoborole intermediate was formed *via* the stannole and BCl_3 followed by the introduction of Mes* on boron using Mes*Li. This intermediate wa stable enough to permit Negishi cross couplings to extend the π-system. Two symmetrically extended boroles were synthesized, with thienyl and *p*(Ph_2N)-phenyl groups, **4** and **5** respectively. The compounds were sufficiently stable to be purified on silica gel. The crystal structure of **4** revealed the molecule was twisted in the solid state, demonstrated by the angles between the plane of the dibenzoborole core and the inner thiophene rings being 5.4° and 31.5°. The extended packing structure showed that molecules are oriented in an offset face-to-face arrangement and the distance of the intermolecular π–stacking is 3.3 Å. Photophysical studies were used to compare the effect of changing the exocyclic group from Mes* to Tip.[9] It is notable that the Mes*-substituted boroles have no solvatochromic character due to the enhanced steric bulk of Mes* which prevents coordination of DMF and even fluoride. **4** and **5** exhibits two absorptions λ_{max}(abs)=388 and 470 nm and λ_{max}(abs)=366 and 457 nm in THF, respectively, with the thiophene moieties on the framework having a bathochromic effect on the spectra compared to the *p*-(Ph_2N)-phenyl analogues. Theoretical calculations (TD-DFT (B3LYP/6-31G(d)) determined that the HOMO is distributed over the complete π-conjugated skeleton for **4** and **5**. The LUMO is principally situated on the dibenzoborole unit with a large contribution from the p_z orbital of the boron centre while the LUMO+1 is also associated with the orbitals delocalised over the entire π scaffold. The shorter wavelength absorptions were attributed to HOMO→LUMO+1 (π–π*) and the longer wavelengths were assigned to HOMO→LUMO (π-(p_π -π*)). Compound **4** displayed two reversible reduction potentials: $E_{1/2}$ =-2.04 and -2.70 V in THF *vs* Fc/Fc^+, generating a stable radical anion and a stable dianion. The dibenzoborole **5** displayed two reductive and two oxidative systems: $E_{1/2}$=-2.19V and E_{pc}=-3.00V; $E_{1/2}$=0.29 and 0.51 V. The first reversible reduction of **4** was shifted about 0.15 V to a less negative potential compare to **5**. The enhanced steric bulk afforded by the Mes* groups also proved essential for reversible redox behaviour.

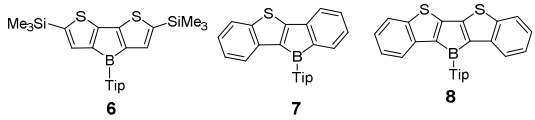

More recently the same group prepared a family of ladder structures with fused thiophene and phenyl groups annulated to the borole core.[11] The synthesis of **6** involved the initial reaction of TipMgBr with the 3'-bromo-2,2'-bithienyl-3-boronic ester, the bromo intermediate tolerated subsequent lithiation with *t*BuLi, which led to ring closure and formation of the borole. **7** and **8** were synthesised starting from an arylalkynyl boronic ester with

initial installation of Tip onto the boron atom again using TipMgBr. A subsequent lithiation step was followed by reaction with S_8 to introduce the sulphur atom and cyclise to form the four-fused-ring **7** and the five-fused-ring **8**, in moderate yields. An X-ray diffraction study of **8** indicated an extremely small deviation from planarity of the outer phenyl groups relative to the borole centre, 2.00(14)° and 4.25(15)°. Contrary to dibenzoboroles **1**, **2** and **3**, the heteroaromatic annulated compounds **6**, **7** and **8** are not sufficiently stable to be purified on silica gel. This difference was attributed to the increased antiaromatic character of **6**, **7** and **8**, which was contrary to the expected effect of fused heteroarene rings decreasing antiaromatic character of 4π electron systems.[12] Based on the methyne chemical shift of the *ortho*-isopropyl of the Tip group, the downfield shifts increased in the order **3<2<7<6<8**, indicating that thiophene fused structures enhanced the antiaromaticity of the borole moiety relative to **2** and **3**. Compared to dibenzoborole $\mathbf{9_{TIP}}$ (λ_{abs}=410 nm),[13] the absorption maxima of **6**, **7** and **8** were red-shifted, (λ_{abs}=552, 469 and 600 nm, respectively). The presence of two fused thienyl groups on a borole core (**6** and **8**) gives rise to a more pronounced bathochromic effect than the mixed fused-phenyl-thienyl borole system of **7**. Two reductions each were observed for **6** – **9**, the first reversible and the second irreversible. For the fused-boroles, **6** - **8**, the reduction occurs at less negative potentials than for $\mathbf{9_{TIP}}$ ($E_{1/2}$=-2.11V *vs* Fc/Fc$^+$) by between 130mV to 390mV for the first reduction and 160mV to 440mV for the second, irreversible reduction. Calculations revealed that the HOMO levels of **6**, **7** and **8** are all higher in energy than the HOMO of $\mathbf{9_{TIP}}$ (due to the more electron rich heteroaromatic) and at the same time the LUMOs are lower in energy for each relative to that of $\mathbf{9_{TIP}}$ consistent with the electrochemistry and the greater borole antiaromaticity with thienyl fusion relative to benzannulation.

With the aim to understand the factors controlling antiaromaticity in fused boroles, Yamaguchi *et al.* investigated a series of boroles fused with the heteroaromatics, pyrrole (**10**), furan (**11**) and thiophene (**12**), which were all synthesised using related pathways to that reported for **6**.[14] Solid state structures and *nucleus independent chemical shift (NICS),* specifically NICS(1)$_{zz}$, calculations confirmed that all three heteroarene fused boroles have increased antiaromaticity relative to C_4H_4BH, in contrast to benzo fused boroles which reduce antiaromaticity. In boroles antiaromaticity can be reduced by increasing the C-C bond length alternation. The authors therefore conclude that the lower C-C bond distance alternations observed for the boracycle in **10** – **12** relative to parent borole lead to enhanced antiaromaticity.[15] However, the dibenzoborole **9** also has reduced C-C bond distance alternation, but a lower antiaromaticity, relative to C_4H_4BH (by NICS(1)$_{zz}$), therefore other factors must also contribute significantly, presumably this includes the aromaticity stabilisation energy of the annulated aromatic, with benzene > the three heterocycles studied. The optoelectronic properties of the fused boroles **10**, **11** and **12** showed similar absorption maximas of 479, 468, and 474 nm, whilst electrochemical investigations revealed that the first reversible reduction potentials shifted to less negative values in the order of pyrrole-fused **10** (-2.25 V) < furan-fused **11** (-1.97 V) < thiophene-fused **12** (-1.89 V) and the oxidation process shows the same trend, **10** (+0.62 V) < **11** (+0.76 V) < **12** (+0.95 V). Theoretical calculations (B3LYP/6-31G*) showed the same trend for the HOMO and the LUMO levels. The change in the chemical shifts of Et_3PO in the ^{31}P NMR spectra on addition to **11** and **12** was small, slightly downfield by 3.6 and 4.2 ppm, respectively, demonstrating the formation of a weak Lewis adduct.[16] The molecule **10** possessed considerably lower Lewis acidity towards Et_3P=O consistent with it having the highest LUMO energy, both indicating that pyrrole is the most electron donating heteroaromatic of the three. This study concluded that the Lewis acidity of the heteroarene-fused boroles is strongly correlated to the energy of the LUMO but less with antiaromaticity.

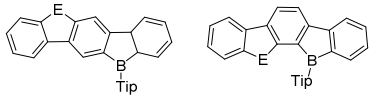

13-Me E= NMe
13-Ph E = NPh
15 E = S

14 E = NMe
16 E = S

More recently, Zhao and co-workers described the synthesis of borole containing ladder structures fused with carbazoles.[17] Two isomers, **13** and **14**, were produced, both formed due to the Cadogan cyclisation step leading to two products. The isomers proved moderately tolerant towards air and moisture, however a crystal structure of a hydrolysed material was reported and assigned as a decomposition product derived from **14**. The photophysical studies revealed large Stokes shifts: **13-Me**, Δλ = 99 nm; **13-Ph**, Δλ = 97 nm; **14**, Δλ = 86 nm. The same group recently synthesised the sulphur analogues, **15** and **16**. The sulphur congeners were found to have increased fluorescence efficiency and larger band gaps than **13** and **14** principally due to a reduction in the HOMO energy.[18]

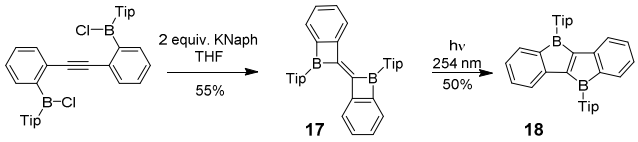

Scheme 2

Piers *et al.* reported a ladder structure containing two annulated borole units.[19] The key precursor was accessed by the double borylation of a di(2-bromoaryl)acetylene using lithium/halogen exchange, stannylation then addition of an excess of BCl_3 and finally installation of Tip on boron using Cu(Tip). Under reductive conditions the bis-benzocycloborabutylidene **17** is formed which on irradiation produces the air- and moisture-sensitive diborole ladder compound **18** in a moderate yield (Scheme 2). A photoinduced homolytic cleavage of the B-C bond between the boron atom and the phenyl group from the butadiene ring is proposed to allow the formation of **18**. Compounds **17** and **18** both possess 14 π electrons and a range of NICS calculations indicated an antiaromatic character for the borole rings with the benzene rings remaining aromatic. UV/vis spectra for compound **17** exhibited two strong absorptions at 263nm, 314nm and a weaker absorption at 459nm. In an elegant follow up report alternative isomerisation conditions for converting **17** to **18** were developed proceeding *via* the di-reduced compound $\mathbf{17\text{-}K_2}$,

formed from addition of potassium naphthalenide to **17**.[20] Guided by acid induced rearrangements in isoelectronic neutral carbon analogues the addition of a Brønsted acid to **17-K$_2$** led to the transformation into **18-K$_2$** which on oxidation using silver triflate yielded **18**. The radical anions, **17-K** and **18-K** could also be isolated and were characterized by EPR spectroscopy, which showed hyperfine coupling to the iso-propyl methine protons of the Tip substituent for both radicals, again indicating that these protons interact with the planar π system.

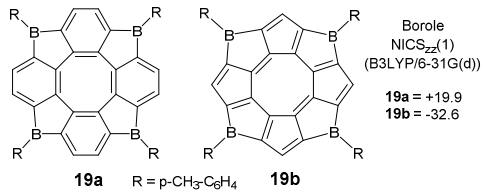

The neutral borole containing ladder structures reported to date all contain antiaromatic five membered boracycles (by NICS calculations). Recent calculations on cyclic fused structures indicate that it is theoretically possible to generate systems where the embedded borole units are actually aromatic based on NICS(1). For example, whereas **19a** contains antiaromatic boracycles (at the B3LYP/6-31G(d) level) **19b** has negative NICS(1) values for both the carbacycles and boracycles making it an intriguing target for future synthetic efforts.[21]

Diboraanthracene and other dibora-acenes

9,10-dihydro-9,10-diboraanthracene (DBA) contains a 6-membered ring with boron atoms at the 1,4 positions annulated by two benzene rings. The interest in this diboracycle derives from its use as a rigid framework to engender luminescent properties and electrochemical reversibility.[22] Whilst the first DBA derivative was synthesised by Clément in 1965 by the reaction between diphenylenedimercury and BCl_3,[23] the most prevalent methods to form 9,10-halo-9,10-dihydrobora-acenes involves the condensation of 1,2-bis(haloboranyl)benzene,[24] or transmetallation from stannyl[25] or silyl precursors.[26] The Lewis acidity of perfluorinated DBAs (e.g., **20**),[27] have been studied through the relative affinity of an acetonitrile molecule towards **20** and $B(C_6F_5)_3$ in toluene-d$_8$ (Scheme 3) which indicated that **20** is a stronger boron-based Lewis acid than $B(C_6F_5)_3$ towards MeCN.[27]

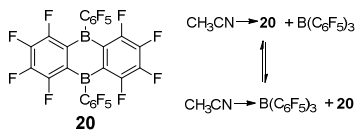

Scheme 3

In a review on aryl(hydro)boranes Wagner and co-workers highlighted that DBA hydroboranes can be considered as starting materials for the extension of boron-doped π-systems.[28] They showed that the hydrogen substituent in aryl(hydro)boranes leads to unique reactivity due to: 1) its small size not hindering dimerisation; 2) its lack of π donor capacity confers to the boron centre high Lewis acidic character; 3) the intermolecular B-H-B bond is easy to form and this lowers the barrier to subsequent B-C-B bond formation. The same group also introduced a method to obtain dihydroboraanthracene polymers starting from 9,10-dibromo-9,10-diboraanthracene[29,30] *via* reaction with an excess of $HSiEt_3$ to give a B-H-B bridged polymer. These polymers can be added to terminal alkynes or a range of diynes to form functionalised vinylborane monomers or polymers.[31]

Kawashima *et al.* described another synthetic route to DBAs, using 1-bromo-2-iodobenzene as a dihalogenated starting material. Multiple metalation / borylation steps led to the borinic ester precursor,[32] which on reaction with mesityl Grignard produced **21**. The obtained crystal structure of **21** shows a B-C(exocyclic) bond length of 1.589(2) Å. Moreover, a low degree of bond length alternation (1.39-1.43 Å) indicated a low degree of π-electron delocalisation over the diboron heterocycle. The NICS(1) value of a model compound of **21** (2,6-dimethylphenyl groups instead of mesityl groups) gave a value of +3.5 for the central C_4B_2 diboron ring indicating weak anti-aromaticity.

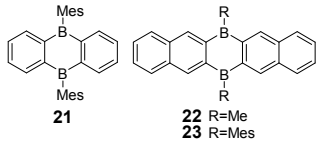

Pursuing the extension of the DBA family further, Ashe and co-workers synthesised a diborapentacene, albeit in low yield,[33] from heating 2,3-bis(trimethysilyl)naphthalene in toluene in presence of BBr_3, presumably *via* the formation a BBr_2-$SiMe_3$ naphthalene intermediate followed by condensation.[26] The initial dibromo substituted diborapentacene was functionalised at boron by the introduction of methyl or mesityl groups, and as expected, the mesityl group provides more kinetic stabilisation. The structures of DBA **22** and **23** emphasised the weak antiaromatic nature of the C_4B_2 ring with B-C bonds (1.54-1.56 Å) only marginally longer than those in boron molecules with a degree of aromatic character (range 1.48-1.52 Å).[34] Compound **22** adopted a packing structure with a face-to-face conformation with an intermolecular distance of 3.50 Å, whereas the Mes congener **23** did not exhibit any similar π-stacking due to the bulky mesityl group. UV-Vis spectroscopic analysis of **23** revealed a small Stokes shift ($\lambda_{abs(max)}$=407 nm; λ_{em}=410 nm), consistent with a rigid molecule. In comparison the photophysical properties of **21** revealed an absorption at λ_{max}=349 nm (π–π*) and a shoulder at λ=400 nm (attributed to intramolecular charge transfer from Mes groups to DBA) in THF and cyclohexane, slightly blue-shifted relative to **23**, due to the less extended π-system of **21**. The emission of **21** was solvent-dependent with a small Stokes shift in cyclohexane (λ_{em} = 413 nm), but red-shifted in THF with λ_{em} = 483 nm. This was interpreted as the emissive state being significantly polarised. Investigation of the Lewis acid character of **22** *via* the binding of fluoride ions (K=2(1) $10^8 M^{-1}$) showed that the fluoride adduct exhibited a blue-shift of the band at λ_{max}=349nm to λ_{max}=280nm and a hypsochromic effect was also observed in fluorescence from λ_{em}= 483 to 400 nm. This new band was attributed to an intramolecular charge transfer between the fluoride anion and the boron moiety.

Comparison of boracycles **21** – **23** with the carbon analogues

was informative. Whilst the optical band gap of **23** (3.0 eV) is larger than that of the pentacene (2.07 eV)[35] the electrochemical data showed that the first reversible reduction of **23** (-1.23 V in acetonitrile) occurred at a less negative potential than pentacene (-1.87 V) as expected due to the electron deficiency of boron.[35] The NICS calculations on $[Li_2(THF)_2]_2$**21** and its isoelectronic anthracene analogue showed only a slight difference (-9.0 ppm/-13.1 ppm *vs* -9.9 ppm/-11.1 ppm, respectively) which was used to suggest that the dianion of **21** has significant aromatic character. Contrary to the dianion, neutral **21** possesses an anti-aromatic diboron ring (NICS(0)/NICS(1) =10.5 ppm / 4.4 ppm, respectively).[32]

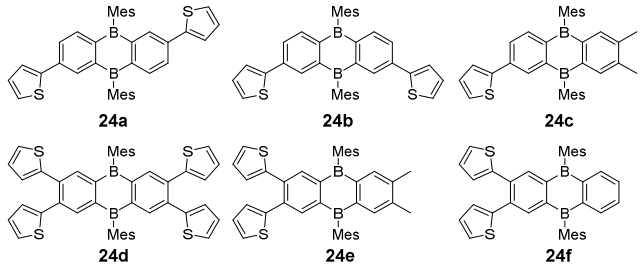

Wagner and co-workers subsequently developed DBA systems functionalised with heteroaromatics to generate more extended structures.[36] This utilised substituted $DBA(Mes)_2$, which proved to be rare examples of a boron centre substituted by only a single mesityl being bench stable, this stability enabled compatibility with some palladium coupling protocols. The synthesis of halogenated $DBA(Mes)_2$ started with a halo-phenylene-bis(trimethylsilane) which reacted with an excess of BBr_3 to obtain halo-phenylene-(BBr_2)-(TMS). Heating the reaction medium to 120°C forms the halo-C_6H_3-$(BBr_2)_2$ intermediate which undergoes subsequent condensation to produce the halogenated DBA which can be mesitylated readily. A $[Pd(PtBu_3)_2]$ catalysed Stille coupling with $PhSnBu_3$, thienyl$SnBu_3$ or Ph_2N-C_6H_4-$SnBu_3$ was then used to produce **24**.

Several thienyl-DBA compounds were crystallised and comparison between the B-C bonds in the diboron ring showed little variation (1.559(9) Å for **24a**, 1.576(6) Å for **24d** and 1.562(3) Å for **23f**). This suggested that thiophene substitution has minimal influence on the central diboron ring and only a weak π-electron delocalisation involving the thiophene rings and the DBA system. However, electrochemical studies on the thiophene substituted DBAs indicated that the more thiophene groups that are appended, the more facile the reduction (**24c** : $E_{1/2}$= -1.83V; **24a**: $E_{1/2}$= -1.71V; **24f**: $E_{1/2}$= -1.62V; **24d**: $E_{1/2}$= -1.59V, *vs* Fc/Fc^+). The effect of varying the aromatic substituent was probed using diphenylaminophenyl substituents. Compounds **25 a-c** possessed a more negative reduction potential than their thienyl congeners (e.g., **25c** $E_{1/2}$ = -1.86 V) and also two irreversible oxidative events.

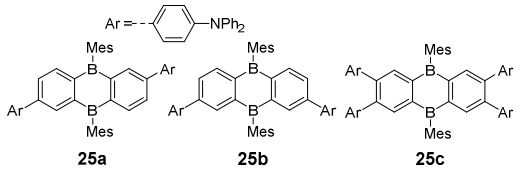

Contrary to the all carbon analogues which are highly fluorescent, the $DBA(Mes)_2$ compounds all displayed limited fluorescence. If the fluorescence of anthryl compounds is attributed to the π–π* transition, the DBA emissions are assigned to intramolecular charge transfer transitions between the orthogonal DBA core and exocyclic mesityl units. Concerning the introduction of moderately electron-donating 2-thienyl groups onto the $(Mes)_2DBA$ framework, the fluorescence changes according to the position and the degree of substitution. Increasing the number of thiophenes induced red-shifted emissions: (**24c** (λ_{em} = 469nm) < **24a/24e/24f** (λ_{em} = 490/515/524nm) <**24d** (λ_{em} = 540nm). Whilst changing the position of the substitution affected the quantum yield: **24a** (ϕ_f = 45%) and **24f** (ϕ_f = 70%). Depending on the number and the position of substitutions, the emissions can be tuned therefore from blue to orange, whereas the all-carbon backbone analogues emit in the near-ultra-violet to blue range, clearly demonstrating the lower band gap achieved by boron incorporation.

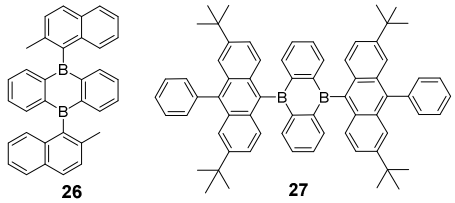

A series of DBA compounds with other bulky substituents on the boron atom has also been studied by Wagner and co-workers.[37] The synthesis of these compounds starts from 9,10-dibromo-DBA, with (2-methylnaphthyl)-DBA, **26**, formed from reaction with the corresponding Grignard reagent, whereas the 9-phenyl-2,7-di-tert-butylanthracene-DBA **27** is obtained using the lithium anthracene derivative. Concerning the electrochemical data, **21**, **26** and **27** all presented two-reversible reductions at $E_{1/2}$= -1.82/-2.78 V, -1.72/-2.58 V and -1.68 /-2.46, respectively in THF (*vs* Fc/Fc^+). The reversible redox waves of **27** were attributed to successive reductions of the DBA fragment whilst a third irreversible redox wave observed for **27** (E_{pc} = -3.32 V) is assigned the reduction of anthryl moiety. The photophysical data exhibited bathochromic shifts in absorption in benzene as the exocyclic aromatic substituents became more extended: λ_{max}(**21**) = 349 nm, λ_{max}(**26**) = 357 nm and λ_{max}(**27**) = 374 nm. Contrary to the all-carbon analogues, which emit in the blue, these DBA derivatives have emissions spanning blue (λ_{em}(**21**)=460nm), green (λ_{em}(**26**)=513nm) and red (λ_{em}(**27**)=635nm). The DBA compounds also displayed solvatochromic behaviour with calculations revealing charge transfer in these transitions with the HOMOs of **21**, **26** and **27** localised on the exocyclic aryl substituents whereas the LUMOs are predominantly localised on the DBA moiety. In contrast, both the HOMO and LUMO of the all-carbon analogues are located on the anthracene centre with no exocyclic contribution.

Substituted anthracene groups were also appended onto the DBA core linked through the boron atoms.[38] The electronic properties were probed by the introduction of phenyl-anthryl, dimesitylborylanthryl (Mes_2B-anthryl) and *N,N*-di-(p-tolyl)amino-anthryl (Tol_2N-anthryl) groups on the boron atoms,

as neutral, electron-withdrawing and electron-donating substituents, respectively. The compounds **28** and **29** were obtained by the lithiation of their bromoanthryl-derivatives followed by the reaction with 9,10-dibromo-DBA. The B-C(exocyclic) bond lengths of **28** are 1.589(4) and 1.581Å(4) Å which is similar to the exocyclic B-C bond length for **21** (1.589(2) Å).[32] The DBA moiety is planar and the dihedral angles between the DBA core and the anthryl moieties are 80.6(2)° and 88.5(1)°. Compound **28** displayed three reversible reductions and an irreversible reduction: $E_{1/2}$=-1.70V, -2.37V and -2.64V and E_{pc}=-3.11 V *vs* Fc/Fc$^+$ in THF, respectively. Compound **29** had two reversible reductions at $E_{1/2}$=-1.69 V and 2.42V *vs* Fc/Fc$^+$ in THF, and two irreversible reductions at E_{pc}=-3.27 and -3.39 V *vs* Fc/Fc$^+$ in THF. The first reductive redox event for **28** and **29** is assigned to the reduction of the DBA fragment and the second for **28** is attributed to the Mes_2B-anthryl substituents. The UV-Vis spectra of **28** and **29** showed two strong absorption bands at λ_{max}= 346, 442 nm and λ_{max}= 359, 429 nm in benzene, respectively (**27**: λ_{max} = 374 nm in benzene) and a charge-transfer band at λ_{max}=536 and 556 nm, respectively (**27**: λ_{max}= 531 nm). Compounds **27** and **28** exhibited fluorescence in benzene solutions at λ_{em}= 635 nm for **27** and λ_{em}= 644nm for **28** (ϕ=0.06), whereas **29** fluoresced only in the solid state with λ_{em}= 675 nm. Mes_2B is a π-electron-withdrawing group thus lowers the energy of the LUMO localised on anthryl. However, as the charge transfer proceeds from the anthryl HOMO into the DBA LUMO the maxima of absorption are similar for **27** and **28**. The small red-shift of **29** relative to **28** is due to Tol_2N substituents which increased the HOMO levels of the anthryl moieties. The electronic spectra of **27**-**29** were described in terms of twisted intramolecular charge-transfer interactions between anthryl donors and DBA acceptors.

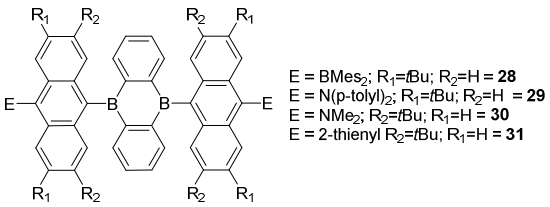

The incorporation of *tert*-butyl groups on the anthryl substituents increased the stability of the boron centres towards moisture and other reagents whilst enhancing the solubility of the framework in non-polar solvents. 9,10-Dianthryl substituted DBA compounds react with *N*-bromosuccinimide / $FeCl_3$ by bromination of the anthryl framework, allowing the extension of the backbone *via* Pd catalysed couplings. [39] The substitution of bromide by NMe_2 or thiophene is achieved using catalytic $[Pd(PtBu_3)_2]$ in presence of Me_3Sn-NMe_2 or nBu_3Sn-thiophene, respectively. The solid state structures of the Me_2N-anthryl-DBA, **30**, and thienyl-anthryl-DBA, **31** have B-C(exocyclic) bonds of 1.575(4) and 1.589(3) Å, respectively. The fact that these lengths are similar to unsubstituted 9,10-dianthryl-DBA (1.557(7)) and Mes_2DBA (1.589(2) Å)[32] was used to conclude that the presence of the Me_2N substituents have little influence on the B-C(exocyclic) bond length consistent with their orthogonal disposition. The Me_2N groups in **30** adopt an angle approximatively 60° relative to anthracene whereas the thiophene analogue is more twisted with an equivalent angle of approximately 80° in **31**, minimizing π conjugation to these substituents. Compound **30** displayed an irreversible oxidation at 0.23V *vs* Fc/Fc$^+$ in electrochemical studies. It also possessed two reversible cathodic systems $E_{1/2}$=-1.77 and -2.60V, assigned as DBA-centred, and an irreversible cathodic wave E_{pc}=-3.30V. The latter is slightly shifted compared to that of the unsubstituted anthryl-DBA (E_{pc}=-3.21V) due to the weak positive mesomeric (+*M*) effect of Me_2N in **30**. In contrast to **30**, compound **31** possesses only cathodic systems (two reversible and two irreversible) and is easier to reduce: $E_{1/2}$=-1.69 and -2.50V; E_{pc}=-3.10 and -3.40V. The photophysical properties of **30** and **31** are similar for the shorter wavelength absorptions (λ_{max}(**30**) =371nm and λ_{max}(**31**)= 373nm in cyclohexane), which were attributed to a local π–π* electronic transition within the anthryl systems. A lower energy broad absorption is situated at 557nm for **31** and is red-shifted to 567nm for **30**, it was attributed to the charge-transfer transition from the more electron-rich anthryl donor to the electron-poor DBA acceptor. Compound **31** is fluorescent (λ_{em}= 582nm) whereas **30** is not due to the quenching effect of the amine group.

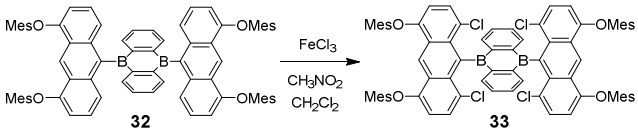

A novel method to modify the 9,10-dianthryl substituted DBA frameworks is to fully-fuse these structures by oxidative C-C coupling the central fused core with the exocyclic substituents. Yamaguchi and co-workers attempted to fuse exocyclic anthracenes to the DBA core for **32**,[40] however, **32** instead reacts with an excess of $FeCl_3$ in CH_2Cl_2/CH_3NO_2 by chlorination instead of the desired oxidative fusion. Significantly, the chlorinated compound, **33**, had an ^{11}B NMR chemical shift of 49 ppm significantly shielded relative to **32**. The crystal structure of **33** revealed that the anthracene groups are almost perpendicular (87.1°) to the DBA core with B-Cl distances shorter (2.707(4) and 2.727 (4)Å) than the sum of the van der Waals radii (3.67Å), but longer than typical B-Cl covalent bonds (1.84 Å). The external B-$C_{anthrancyl}$ (1.609(5)Å) bonds in **33** are also elongated compared to those in **32** (1.560(4) and 1.581(4)Å). Combined the data indicated a penta-coordinate boron atom in **33**, which was supported by extensive computational studies. The photophysical properties of **32** displayed an intense absorption band showing distinct vibronic structure at 409 nm, and a weaker broad band at 522 nm whereas **33** exhibited a band showing distinct vibronic structure at 432 nm. Introduction of chlorides blue-shifts the fluorescence from λ_{max}(em): 632 nm for **32** to λ_{max}(em): 467 nm for **33**. Electrochemical analysis revealed two reversible reductions for **32**: -1.68 and -2.48 V *vs* Fc/Fc$^+$ in THF; and a quasi-reversible oxidation at 0.61 V *vs* Fc/Fc$^+$ in CH_2Cl_2. **33** exhibited distinct behaviour possessing two reversible oxidation processes more positive than **32**: $E_{1/2}$: 0.70 and 0.79 V *vs* Fc/Fc$^+$ in CH_2Cl_2 and three irreversible reductions more negative than **32**: E_{pc}=-2.23, -2.43 and -2.64 V *vs* Fc/Fc$^+$ in THF. The theoretical calculations highlighted that an antibonding interaction on chlorination of the anthracene moieties elevates the p-π* molecular orbital of the DBA core and is the dominant cause of the changes in the photophysical and electrochemical behaviour.

Fully fused (di)boraanthracenes and derivatives

Yamaguchi and co-workersinvestigated the full fusion of the bora-acene- scaffold which will lock the boron centre in a planar geometry to "kinetically" stabilize the boron centre against pyramidilisation and thus nucleophilic attack. In addition to imparting structural constraint to the molecule planarization will facilitate intermolecular interactions (e.g., π stacking) that are required for effective charge transport. Recently, Yamaguchi and co-workers synthesised the fully fused boron containing poly aromatic hydrocarbon,[41] derived from a diborapentacene with anthracenes attached at boron for subsequent fusion.[42] Scholl oxidation was used, to fully fuse the molecule **34** to produce **35** (Scheme 4).

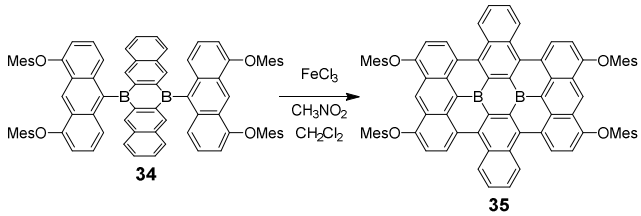

Scheme 4

Fully fused **35** is sufficiently stable to be isolated on silica gel without special precautions. It was isolated as a crystalline solid and X-ray structural analysis showed a slightly twisted conformation, with an angle of 19.7° between the plane of the most deviated benzene ring and the plane of the central C_4B_2 moiety. The B-C bond lengths are shorter in **35** (1.53 Å and 1.51 Å) than the unfused mesityl substituted diborapentacene **23** (1.56 Å, and 1.58 Å). No π-stacking is observed in **35** due to the presence of the solubilising mesityl groups which are orientated perpendicular to the main skeleton of **35**. The photophysical properties revealed that the absorption of **35** is significantly red-shifted compared to **23**. Compound **35** was not solvatochromic (in THF, CH_2Cl_2 and toluene) and has an extended absorption in the visible region from 400 to 700 nm with λ_{max}= 564 and 487nm (HOMO-1→LUMO+1 and HOMO-2→LUMO, respectively, assigned by TD-DFT (B3LYP/6-31G*)) and a shoulder at 640nm (HOMO→LUMO). Compound **35** is red-shifted relative to hexabenzocoronene (λ_{abs} =361 and 392 nm) but blue-shifted relative to teranthene (λ_{abs} =878 and 1054 nm). The fluorescence spectrum of **35** showed a broad band in the visible / near-IR region at λ_{max}(em) = 679 nm with a low quantum yield ($\phi\varphi$ = 0.04). Electrochemical studies showed that **35** possesses a reversible oxidation at 0.62V in THF *vs* Fc/Fc^+ and two reversible reductions at $E_{1/2}$ = -1.45 and -1.66V in THF *vs* Fc/Fc^+. Two reversible reductions were also observed for **35** in CH_2Cl_2, whereas only one reversible reduction was observed with the unfused DBA **23** in acetonitrile at -1.23V.

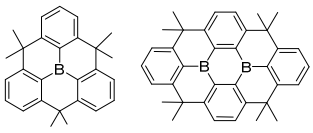

An alternative strategy to access fully fused planar at boron molecules utilised Friedel-Crafts chemistry.[42] This approach was used to prepare **36** and **37** containing one and two boron atoms, respectively. Borane **36** was synthesised from 9-bromo-9,10-dihydro-9-boraanthracene which reacts with 2-lithium-1,3-di(propen-2-yl)benzene to give the key precursor for cyclisation which is achieved using $Sc(OTf)_3$. Remarkably, the methylene tether can then be oxidised with CrO_3 (in HOAc, 120°C) without any reactivity at the boron moiety. The oxidised intermediate was treated with $ZnMe_2$ and $TiCl_4$ to give the symmetrical fused molecule **36**. The same cyclisation methodology was applied to obtain **37**. X-ray crystallography revealed effectively planar solid state structures with deviations away from planarity that were extremely minor (0.0-0.15° and 0.0-2.6° for **36** and **37**, respectively). The B-C_{ipso} bonds (1.520(2) - 1.532(2)°) for **37** are shorter than for non-fused DBAs (e.g., for **21**, 1.54-1.58°), but similar to **35**. The C_{ipso}-B-C_{ipso} angles were all close to 120°. Previously, a related substituted and fused triphenylborane was synthesised by Okada and Oda with longer linkers of $–CH_2CH_2$- (versus $–C(Me_2)$- in **36**).[43] In contrast to **36**, ethylene linkers led to three fused seven membered rings around the central boron, thus the molecule deviates significantly from planarity.

The spectroscopic data show an effective extension of π conjugation for **37** containing two boron centres with bathochromic shifts for the absorptions of **36** relative to **37**: λ_{max}(abs)= 289, 310 (sh), 320 (sh) nm and λ_{max}(abs)= 377 nm in THF, respectively. Compound **37** is also red-shifted compared to **21** by 28 nm. The emission of **37** was red-shifted relative to **36**: λ_{max}(em) = 407nm and λ_{max}(em) = 384 and 400nm, respectively. Even though the planar structures are fully fused, the methylene tethers permit a degree of flexibility to the framework. As a consequence the planarised **36** displayed two emissions, one from the planar excited state at 337 nm, observed at low temperature, and a second one from a bowl-shaped excited state at 407 nm.[44] The HOMO and HOMO-1 are delocalised on the benzene moieties of **36** while the LUMO resides principally on the vacant p orbital on the boron atom. It was reported that intramolecular charge transfer, from the benzene moiety to the boron centre on excitation, causes an elongation of a B-C bond and breaks the planarization to allow a pyramidal conformation at boron and an overall bowl-shaped to the molecule.

Electrochemical studies on **36** and **37** revealed fully reversible cathodic systems confirming the high stability of the planarised boron-containing skeleton under these conditions even without bulky protecting groups on the boron atom.[41] **36** showed one reversible wave at $E_{1/2}$=-2.59V, in THF *vs* Fc/Fc^+, which is less negative than Mes_3B $E_{1/2}$=-2.90V in THF.[45] The crystal structure of the radical anion, $\mathbf{36}^{\bullet-}$, formed during the reduction process also adopts a bowl-shaped conformation.[46] Compound **37** displayed two reversible cathodic waves at $E_{1/2}$= -2.04 and -2.56 V, in THF *vs* Fc/Fc^+, where the first reduction occurs at a less negative potential than **36**. The Lewis acidities of the fused monoborane **36** and diborane **37** were also studied, with a notable result being that **36** did not bind amines such as DBU or DABCO, but it did react with the fluoride sources, e.g., $[Me_3SiF_2]^-[S(NMe_2)_3]^+$ (TSAF) in THF. The X-ray crystallographic analysis of $\mathbf{36F^-}$ revealed a bowl-shaped structure. The molecule $\mathbf{37(F^-)_2}$ was also structurally characterised and adopted a concave shape with both fluoride

ions bound to the same face of molecule. This was calculated as the thermodynamically more stable isomer by 6.7 kcal/mol over the *trans*-fluoride isomer. The depth of the concave structure of **37(F⁻)$_2$** (2.49 Å) is 0.84 Å deeper than **36F⁻** (1.65 Å). Fluoride binding and the concomitant structural change can be reversed by addition a fluorophilic Lewis acid such as $BF_3.Et_2O$.

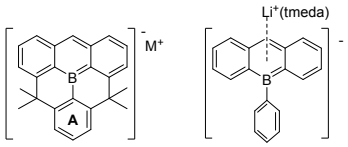

38.K (M⁺=K⁺([2.2.2]cryptand)
38.Li (M⁺=Li⁺(thf)$_4$)
39.Li

After obtaining planarised neutral boron-containing molecules, Yamaguchi and collaborators studied the planarisation of anionic fused boracycles.[47] Compound **38** may be prepared from an intermediate *enroute* to **36**. Following its cyclisation with $Sc(OTf)_3$ but before oxidation the intermediate can be deprotonated with KH (with K sequestered subsequently with [2.2.2]cryptand), or alternatively using lithium tetramethylpiperidine (LiTMP). The crystal structures of **38.K** and **38.Li** show that neither the cation, K^+ (ligated by the cryptand) nor Li^+ (coordinated by four molecules of THF), interact significantly with the fused phenylborataanthracene anion. The weakly coordinating nature of **38⁻** is attributed to the delocalisation of the charge throughout the entire planarised moiety. The structure of the anion is effectively planar with only a minor twist, for example the angle between the plane defined by B-(C_{ipso})$_3$ and phenyl group **A** is only 5.1°. The ^{11}B NMR chemical shifts of **38.K** (30.0 ppm in THF-d_8) and **38.Li** (30.4 ppm in THF-d_8) are shifted up-field relative to the non-fused **39.Li** albeit in different solvents (39.8 ppm in C_6D_6). The two C-B bonds of the boraanthracene moiety of **38.K** (1.492(7) and 1.495(7) Å) are also significantly shorter than those of the unfused analogue **39.Li** (1.532(3) and 1.549(3) Å). The anion **38.K** exhibits well-defined vibronic structure with λ_{max}(abs) =500, 531 and 568 nm in THF and λ_{max}(em)=584 nm. The aromaticity of the boracycle was computationally assessed producing NICS(1)$_{zz}$ values of -22.6 ppm for **38⁻** and -28.1 ppm for **39⁻**, suggesting that the boracycle in **38⁻** is less aromatic than the analogous boracycle in **39⁻**. This is attributed to different degrees of localisation of the negative charge with charge delocalised over the entire molecule in **38⁻**, while it is delocalised only over the boraanthracene moiety for **39⁻**.

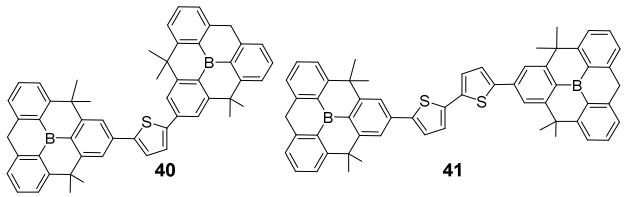

40 **41**

Extended derivatives have also been prepared containing two fully fused boron embedded polyaromatic hydrocarbons connected by thiophene spacers for the purpose of probing the electron-transporting potential of such materials.[48] The fused triarylborane is synthesised using the same methodology as for **36**, but using 9-bromo-9,10-dihydro-9-boraanthracene and 4-bromo-2,6-di-(2-propenyl)phenyllithium as precursors. The planar boron containing components are linked via Suzuki-Miyaura coupling in the presence of the 2,5-thienyl-diboronic ester or the 2,2'-bithiophene-5,5'-diboronic ester, yielding **40** and **41**, respectively. The UV-Vis absorption of compound **41** exhibited a bathochromic shift relative to **40**, due to the extension of π conjugation: **40**: λ_{max}(abs) = 391 nm and **41**: λ_{max}(abs)= 418 nm in THF. The same trend was present in the fluorescence spectra: **40**: λ_{max}(em) = 441 nm and **41**: λ_{max}(em) = 482 nm in THF. The electrochemical data showed reversible redox waves for both compounds with that of **40** occurring at a more positive potential than for **41** for the oxidation process: $E_{1/2}$= 0.90 V and $E_{1/2}$= 0.67 V in CH_2Cl_2 *vs* Fc/Fc⁺, respectively. In addition, **40** exhibited two reversible reduction processes $E_{1/2}$= -2.27 V and -2.35 V, whereas **41** presented only one: and $E_{1/2}$= -2.27 V, both in CH_2Cl_2 *vs* Fc/Fc⁺. This was interpreted as the two boron units being electronically connected to each other by the shorter linker (**40**) but not by the longer linker (**41**). Theoretical calculations (at the B3LYP/6-31G(d) level) suggested that the LUMOs of **40** and **41** are each delocalised over the entire molecule. In contrast, the HOMOs are mainly situated on the bridging diphenylthiophene or diphenyl-bithiophene moieties. The calculated data (**40**: HOMO:-5.39 eV; LUMO:-1.95 eV and **41**: HOMO:-5.14 eV; LUMO:-2.00 eV) indicated that the extension of the bridging π-moiety, through addition of a second thiophene ring, principally affects the HOMO. The X ray crystallographic data showed that **40** adopted a bowed structure whereas **41** was effectively planar. The electron affinities of both **40** and **41** were measured and found to be similar to AlQ_3 (tris(8-hydroxyquinolato)aluminium). OLEDs were constructed using both **40** and **41** and the applied voltage required to give luminance of 1000 cd/m^2 was 7.6 V for **41** and 9.4 V for **40**. These values are notable as they are very close to that of AlQ_3 (7.2 V) suggesting comparable behaviour to this commonly used electroluminescent material.

Yamaguchi and co-workers further explored their planarization at boron concept and utilised benzothiophene moieties to construct fully fused boron centred polycyclic structures.[49] The synthesis of the framework starts with the lithium/iodine exchange of 4-bromo-3-iodobenzothiophene. The lithiated intermediate was then reacted with anthryldimethoxyborane, (with the anthryl moiety containing OMes groups to improve the solubility and to direct the subsequent intramolecular cyclisation). To form **42**, this borane precursor then underwent two consecutive cyclisation steps (Scheme 5) the first radical initiated using (TMS)$_3$SiH and ABCN (ABCN = 1,1'-Azobis(cyclohexanecarbonitrile) to fuse the benzothienyl groups. The moiety was then fused to the benzothiophene C2 positions scaffold *via* Scholl coupling.

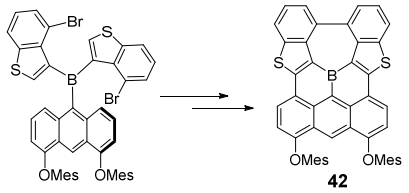

Scheme 5

Compound **42** was found to be highly stable towards air and moisture and only decomposed on only heating to 424°C. The crystal structure of **42** revealed a planar scaffold with only an extremely small deviation of 0.15 Å between the anthracene and the benzothiophene moieties. Importantly for charge transport applications, **42** formed π-stacked dimers in the solid state with an intermolecular distance of 3.53 Å, in contrast to related compounds containing bulky exocyclic groups on boron. Photophysical studies showed a broad absorption in the visible region from 400 to 730 nm, with λ_{max}(abs) = 527, 563, 620 and 668 nm. The absorption was significantly red-shifted compared to **36** due to the relatively electron rich thiophene moieties. **42** fluoresced in the near-Infrared at λ_{max}(em)= 729 nm, albeit with a low quantum yield (ϕ = 0.016). Neither absorption nor emission was found to be solvatochromic. DFT calculations (at the B3LYP/6-31G level) revealed a high lying HOMO, delocalised over the benzothienyl and the mesityloxyphenyl section of the anthracene moiety, while the HOMO-1 is delocalised over entire π-skeleton including the p orbital of the boron atom. The LUMO is mainly situated on the anthracene moiety with a contribution from the p_B-π*interaction. The absorption at 527 nm was assigned to the HOMO-1→LUMO transition and that at 668 nm to the HOMO→LUMO transition. The LUMO of **42** (-2.56 eV) was calculated to be lower than that of **36** (-1.56 eV) consistent with the more facile reduction of compound **42** relative to **36** (**42** shows reversible reduction and oxidation: $E_{1/2}$= -1.37 V and $E_{1/2}$= 0.60V in THF *vs* Fc/Fc$^+$). The Lewis acidity of **42** was studied by reaction with Lewis bases such as fluoride and pyridine. The ^{11}B NMR chemical shift moves up-field from 39.5 to 1.6 ppm in $CDCl_3$ after the addition of Bu_4NF, consistent with adduct formation and formation of a four-coordinate boron atom. The complex-formation equilibrium constant is K=1.3 10^5M^{-1} which is lower than that of **36** (K=7.0 10^5M^{-1}) showing that **42** is less Lewis acidity due to the increased rigidity of the system. The weak Lewis acidity of **42** was confirmed by titration with pyridine (K = 0.35 M^{-1} at room temperature). **42F$^-$** was found to have a nearly planar solid state structure with only a small deviation of the boron atom from the extended planar π-skeleton. The sum of the C-B-C angles in **42F$^-$** was 337.1° corresponding to a tetrahedral structure distorted towards planarity. The smaller deformation on fluoride binding, compared to **36**, was attributed to a greater degree of structural constraint in **42**.

In related work Yamaguchi and co-workers also attempted to synthesise a fully fused tri(benzothiophene)borane, however they only obtained a partially fused stable molecule in low yield (7%) due to difficulties in the cyclisation step.[49] Utilising a related approach the same group synthesised a partially fused naphthylborane, **43**, in improved yield (26 %).[50] The cyclisation reaction of tris(8-bromonaphthyl)borane involved a radical coupling using $(TMS)_3SiH$ and ABCN. The compound was air and moisture stable and could tolerate bromination and subsequent Suzuki-Miyaura coupling conditions to further extend the conjugated scaffold. X-ray analysis of bromide substituted **43** again revealed a planar structure with the boron atom adopting a locally trigonal planar geometry. The B-C bond lengths were longer (1.549-1.603(10) Å) than those of **36** (1.519(2)-1.520(2) Å).[42] The molecule **43-Br** (see scheme 6) formed π-stacked columns in the extended structure with an average intermolecular distance of 3.45 Å. The electron and energy transporting properties were investigated (with hole mobility μ_h= 9.3 10^{-6} cm^2 V^{-1} S^{-1}, and electron mobility μ_e=1.7 10^{-5} cm^2 V^{-1} S^{-1}). Compound **43** was also used to create the first OFET of an air and moisture stable bora-acene.

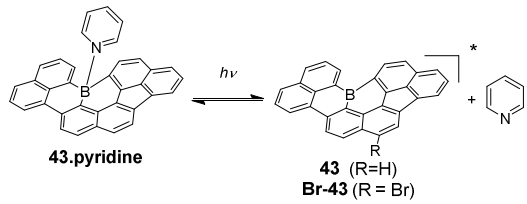

Scheme 6

Electrochemical measurements on **43** showed a reversible reduction at $E_{1/2}$= -1.48 V THF *vs* Fc/Fc$^+$ showing that **43** is more difficult to reduce than **42** ($E_{1/2}$=- 1.37 V). The Lewis acidity of **43** was probed with pyridine, with adduct formation observed. The crystallographic data of two independent molecules of **43.Pyridine** in the solid state structure showed a sum of C-B-C angles of 340.2 and 342.2°, which represent shallow bowl-shaped structures. The Lewis base affinity of **43** was further studied by spectroscopic titration with pyridine in toluene with K = 5.1 10^3 M^{-1}. Compound **43** absorbed at λ_{max}(abs) = 429 and 546 nm in toluene and after addition of pyridine a hypsochromic shift was observed (λ_{max}(abs)= 346 and 374nm, with a broad tail at 490 nm). This was interpreted as the coordination of the pyridine molecule to the formally empty p orbital of the boron atom which has the consequence of disrupting π-conjugation. The fluorescence of **43** was measured λ_{max}(em)= 573nm and found to have a small Stokes shift ($\Delta\lambda$ = 27 nm) and a quantum yield of 0.15. The addition of pyridine decreased the emission intensity of **43** with a band appearing at 500 nm but with the persistence of λ_{max}(em) =573 nm. This phenomenon was attributed to the photo-dissociation of pyridine from **43.Pyridine**, resulting in the observation of emission from both [**43.Pyridine**]* and **43***. The photo-dissociation was dependent on the Lewis base and this double fluorescence occurred only for pyridine and not for derivatives such as 4-DMAP or 3-fluoropyridine.

Fused structures containing borepin moieities

Borepin is an aromatic boron-containing seven-membered ring possessing 6 π-electrons. In 1960, the first fused borepin, dibenzoborepin, was synthesised by van Tamelen,[51] subsequent work predominantly focused on non-fused borepins, including alkyl substituted borepins,[52] which are unstable towards water contrary to isoelectronic tropylium cations,[53] and aryl substituted borepins such as heptaarylborepins.[54] More recently, Piers *et al.* synthesised a series of annulated borepins that included

dibenzoborepin.[55] The borepins were formed via the stannacycles by tin boron exchange and subsequent installation of a mesityl group was as the exocyclic substituent to provide steric protection.

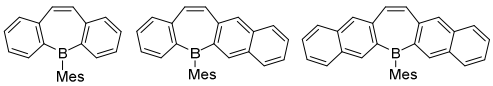

The symmetrical molecules **44** and **46** were found to deviate from planarity in the solid state due to edge-to-face packing interactions, whereas the planar unsymmetric borepin **45** exhibited face-to-face packing. Concerning the electrochemical studies, these borepins have a quasi-reversible reductive behaviour in THF at -2.56, -2.25 and -2.20 V for **44**, **45** and **46**, respectively. The photophysical studies revealed a bathochromic effect as the π-system was extended, with λ_{max} of 260, 280 and 314 nm, respectively. These borepins were all emissive but the blue fluorescence drastically dropped in intensity for **46**. Increasing the conjugation by the introduction of supplementary fused phenyl groups also decreased the band gap, from 3.11 to 2.81 and 2.61 eV for **44**, **45** and **46**, respectively. DFT calculations indicated that for **44** the HOMO and the LUMO are both centred on the boron-carbon backbone, but for more extended **45** and **46**, the HOMO is based on the carbon skeleton while the LUMO has a contribution from boron.

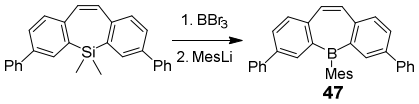

Scheme 7

More recently, Piers, Yamaguchi and co-workers developed alternative synthetic routes to borepins.[56] Instead of using a "stannapin" precursor, they explored the conversion of silepins to borepins. For example, the *meta*-substituted dibenzoborepin **47** with two benzo-fused phenyl groups was prepared from its silepin by reaction with BBr_3 and the resulting bromodibenzoborepin was protected by addition of a mesityl organometallic. This synthetic route to borepins works with the donor substituent $-C_6H_4-NPh_2$ on the core but secondary reactions also occur between BBr_3 and the Lewis basic site.

Another route to functionalized borepins was reported by Yamaguchi and co-workers,[57] and is related to the synthesis of diborole **18** discussed earlier.[19] Compound **48**, stabilised by two lithium cations binding to two oxygens of the boronic ester, is reacted with three equivalents of mesityl Grignard, then water to generate borepin **49** in a high yield (75%) *via* an unusual boratacyclopropene-fused borepin. In solution the borepin **49** displayed reversible photochromic character showing two absorption bands at 346 and 387nm, which decreased in intensity under UV irradiation with a new band observed at 634nm. Colourless **49**, under irradiation at 320nm, formed deep blue **50**, which was crystallographically characterised. During the formation of **50** a new C-C bond is formed between the mesityl group and the double bond of the borepin to form a five-membered ring incorporating a boron atom.[58] The 4π electrocyclization of **49** to form **50** can be viewed as a bora-Nazarov cyclization, with compound **49** isosteric to an intermediate in the Nazarov reaction.

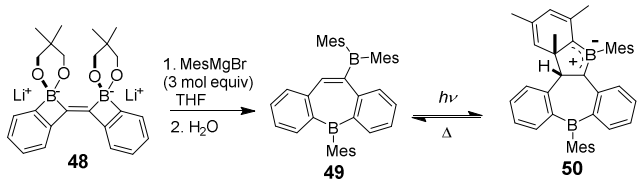

Scheme 8

Regarding other borepins, Tovar and co-workers synthesised multiple borepins again *via* tin intermediates.[59,60,61,62] In this case the borepins are stabilised by installation of the Mes* group using LiMes* (92% from B-Cl, 32% from B-Br). The robustness of the Mes*borepin core allows the extension of the π-scaffold under palladium or nickel cross-coupling conditions (Suzuki, Sonogashira, Stille or Kumada) in moderate to high yield. The first studies concerning extended framework-borepins showed that, the molecules **51**, **52a** and **52b** all possess very similar optical properties but different reduction potentials. This was attributed to the presence of orbital nodes on the aryl-aryl junction that result in the HOMO being localised on the dibenzoborepin core with only minimal delocalisation of the LUMO.[59]

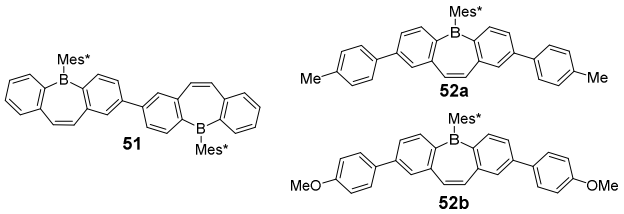

The influence of dibenzoborepin substitution patterns on physical properties was also explored using thiophenes, phenyls and NPh_2 substituents.[60] The computational data indicated a node in the HOMO located on the boron centre for the *para*-(relative to boron) substituted compounds whereas the HOMO of *meta*-functionalised compounds was calculated to be fully delocalised along the entire framework. The cyclic voltammograms exhibited reduction potentials that were less negative for *para* relative to *meta*-substituted compounds. Depending on the substitution of the dibenzoborepin core, the HOMO and LUMO can therefore be selectively tuned: with *meta*-substitution decreasing the band gap while *para*-substitution increasing the electron affinity of the system. Moreover, an analogous functionalization study on the fused *para*- dibenzoborepinobenzene **53** showed that the *meta*-substituted compound is less reactive towards cross-coupling reactions[61] than the *para*-substituted analogue or for dibenzoborepin congeners.[60] The photoluminescence of the dibenzoborepinobenzene **53** was found not to be dependent on the substituents due to the presence of a node between the substituents and the borepin core, which prevents effective electronic delocalisation. A series of functionalised borepin cores with electron-donating (thiophene **53a**, Me_2N-Ph-C≡C **53b**, MeO-Ph-C≡C **53c**), electron-withdrawing (F-Ph-C≡C **53e**,

$EtCO_2$-Ph-C≡C, **53f**) and neutral (Ph-C≡C **53e**) groups on the carbon skeleton were synthesised to tune the LUMO. However, the optical and electrochemical data reveal the same band gap for all analogues, confirming the lack of effective electronic communication.

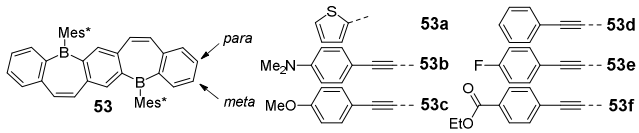

Direct comparison of *meta* and *para* dibenzoborepinobenzene **53** and **54** by UV/Vis spectroscopic analysis revealed a number of differences. The *meta*- dibenzoborepinobenzene **54**[62] exhibited a blue shift compared to the *para*- dibenzoborepinobenzene **53** interpreted as a decrease in electron delocalisation. The quantum yield from **54** was also higher than that found for **53**, which was attributed to the steric demand of the Mes* groups that are closer to each other in **54** than in **53**. This constrains molecule **54** in a more rigid configuration diminishing non-radiative decay processes. While **53** displayed two reversible cathodic events ($E_{1/2}$ = -1.89 and -2.46 V *vs* Ag/Ag^+ in THF), **54** presents a single reversible reduction wave at $E_{1/2}$=-2.12 V, more negative than the first reduction potential of **53**. The backbone **54** was also extended by the introduction of two electron-donating groups at the *para* position (relative to boron), thiophene and Me_2N-Ph-C≡C. For thiophene substituted **54a**, there was no significant difference relative to the unsubstituted dibenzoborepinobenzene (**54**). In contrast, the absorption onset and the fluorescence after the introduction of Me_2N-Ph-C≡C group (λ_{onset}**54b** = 461 nm) are red-shifted relative to unfunctionalised **54** (λ_{onset}**54** = 421nm) attributed to the strong electron-donating nature of the pendant group which raises the "push-pull" character of the chromophore.

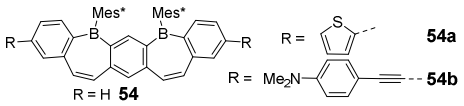

More recently, dithienoborepins were synthesised to further probe substituent effects on opto-electronic properties. Conjugation was found to depend on the functionalization at the α-position of the thiophene, with weak conjugation between R-substituents and boron atom for **55** whereas it is stronger for **56**.[63] The dithienoborepins were prepared from (Z)-dibromodithienylethenes by bromide- lithium exchange followed by the addition of $MesB(OMe)_2$, to form air-and-moisture stable **55** (43%) and **56** (70%). In comparison to the parent dibenzoborepin (NICS(1) = -2.90 ppm), the dithienoborepins were calculated to possess a higher aromatic character (for **55** NICS(1) = -4.93 ppm and for **56** NICS(1) = -4.90 ppm). This was rationalised as the delocalisation of aromatic π-electrons being weaker within the thiophene rings relative to benzene rings facilitating more delocalisation through the central borepin ring. Compounds **55** and **56** were both found to be highly planar with small inter plane thiophene-thiophene angles of 2.4° and 3.0°, respectively with the Mes group approximately perpendicular to the borepin scaffold (76.6° and 82.5°, respectively). Due to the steric constraint of the Mes group, no extended π-stacking was observed. The fused dithienoborepins **55** and **56** had shorter B-$C_{thienyl}$ bonds (B-$C_{thienyl}$ (**55**) = 1.533(2), 1.538(2) Å and B-$C_{thienyl}$ (**56**)= 1.522(2), 1.521(2) Å) than the unfused dithienoborepin (1.544(4), 1.549(6) Å[64]) which indicated an enhancement of π-bonding. Moreover, the B-$C_{thienyl}$ bonds of **56** were significantly shorter than **55**, consistent with stronger π-electron conjugation along the thiophene-boron-thiophene axis in **56** than **55**.

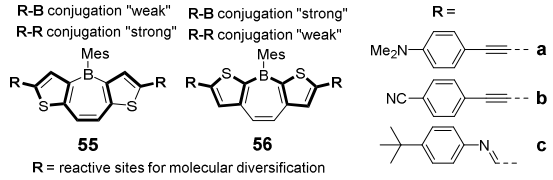

The absorption properties of these systems showed a bathochromic shift for **55** (λ_{onset}= 390 nm) relative to **56** (λ_{onset}= 378 nm). This was attributed to a greater electron delocalisation due to a longer conjugation pathway *via* the olefin bridge of the borepin core compared to the smaller conjugation pathway *via* the boron centre. The electrochemical studies showed that **56** has a higher LUMO energy than **55** (For **55** $E_{1/2\ red}$ = −2.26 V, for **56** $E_{1/2\ red}$= −2.42 V *vs* Ag/Ag^+) which again was consistent with "strong" conjugation with the thienocycles attenuating the electron-deficient character of boron in **56**. **55** and **56** were also functionalised to extend the π system by connecting donor (Me_2N-Ph-C≡C **55a** and **56a**), acceptor (p-CN-C_6H_4 **55b** and **56b**) or imine substituents (**55c** and **56c**). The *p*-CN-C_6H_4 substituted compounds displayed four reversible reductions due to the high electron-acceptor capacity of boryl and *p*-CN-C_6H_4 groups conferring stable tetraanionic states to these molecules. Depending on the isomer and substituents, the effect of fluoride binding on the boron-π–system varied according to the conjugation pathway. For example, for **55a** the carbon conjugation pathway is not affected by the fluoride binding, whereas in **56a** the delocalisation is switched off due to the coordination of F^- to the boron p-orbital. This effect was only observed for the Mes-functionalised congener, which is sufficiently less bulky than Mes* therefore permits fluoride binding.

Fused structures containing heteroborins

The introduction of other main-group elements into π-conjugated ladder molecules in addition to boron has also been investigated. Elements such as nitrogen, sulphur or oxygen are electron donors and on introduction to a carbon framework tend to increase the HOMO energy, which can be a complementary effect to the role of boron in these frameworks (lowering the LUMO).

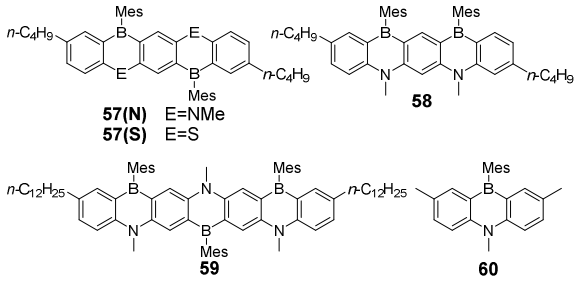

With the aim to reduce the band gap, Kawashima and co-workers investigated ladder-type heteroatom-boracenes (HBAs) which possessed significant rigidity and planar skeletons.[65] The key precursors were synthesised from butylaniline and dihalobenzenes *via* palladium-catalysed amination. These intermediates were then lithiated with *t*BuLi and reacted with $MesB(OMe)_2$ to give the target ladder-type molecules such as **57(N)**. The crystal structure of **57(N)** revealed that the molecule is slightly twisted with a deviation of 9.21° between the two planes, one defined by the central aromatic ring and by the other phenyl rings at the extremities. The photophysical data of **57(N)** and **58** were compared to the more extended ladder-type molecule **59** and to **60**. As expected, the extension of the ladder red-shifts the absorption (**57(N)**: λ_{max}(abs) =523 nm / λ_{max}(em)= 534 nm) (**59**: λ_{max}(abs)= 608 nm / λ_{max}(em) =625 nm), relative to compound **60** (λ_{max}(abs)= 405 nm / λ_{max}(em)= 421 nm). However, this red-shift was less pronounced for **58** (λ_{max}(abs)= 415 nm /λ_{max}(em)=428nm).

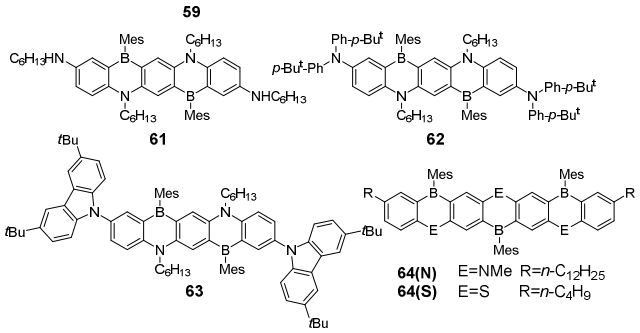

Compound **57** was modified by elongating the alkyl chains on the nitrogen atoms from Me to hexyl, and by replacing the butyl chains with amino groups (**61**: NHC_6H_{13}, **62**: $N(pBu^t\text{-}Ph)_2$ and **63**: (carbazol-$(Bu^t)_2$)).[66] The installation of terminal amino groups again utilised palladium coupling, demonstrating the stability of the boron core to this process. The introduction of amino groups led to a red-shift in the absorption relative to **57(N)**. Compounds **61** and **62** displayed a larger red-shift (λ_{max}(abs) =580 and 568 nm, respectively) relative to **57(N)**, than compound **63** (λ_{max}(abs)=529 nm/(λ_{max}(em)=546 nm, ϕ=0.98). Due to the rigidity of the azaborine and the carbazole components of **63** it exhibits a greater quantum yield than **57(N)**, which was significantly higher than that of **61** (ϕ= 0.12) and **62** (ϕ= 0.20).

The Kawashima group also extended its investigations into ladder-type HBAs by incorporating sulphur atoms in place of NR groups.[67] The X-ray structure of one such compound, **57(S)**, revealed that there is a slight twisted (12.4°) between the central heteroborin ring and the external aryl rings. The absorption of the sulphur congeners (S-DBHs) were blue-shifted relative to the nitrogen based HBAs attributed to S-HBAs having weaker donor-acceptor interactions than the N-HBAs, presumably due to the lower donor strength of S leading to a lower HOMO. The observed trends in the properties of N-HBAs on the extension of the ladder length are similar to that observed for S-HBAs. Fluoride titration studies (TBAF in THF) of **57(N)**, **64(N)** and their sulphur analogues showed that Lewis acidity increased with an extension of the framework. Additionally, the sulphur analogues have higher Lewis acidity then their nitrogen analogues as expected (based on the degree of π donation from the heteroatom) giving the following series of Lewis acidity: **57(N) < 64(N) < 57(S) < 64(S)**.

Kawashima *et al.*[68] compared the effect of nitrogen versus phosphorus as the second bridging main group atom on the Lewis acidity at boron. The crystal structures revealed that the nitrogen-containing **60** is slightly distorted from planarity with a deviation of 9.1° between the two planes defined by each phenyl group of the HBA. In contrast, the equivalent distortion of phosphorus-containing analogue **65** is larger at 15.7°, due to pyramidalisation of the phosphorus atom (sum of the bond angles around P atom: 307°).[69] Moreover, a deviation of 19.7° was observed between the two planes, one defined by five of the six atoms of the HBA central ring, namely boron and the four carbon atoms, and another defined by the phosphorus atom and the adjacent carbon atoms of the central ring. Oxidation of the phosphorus centre with sulphur or selenium afforded **66** and **67,** respectively. The solid state structures included one polymorph of **66** and **67** with a planar central ring and another polymorph of **66** and **67** with a degree of distortion from planarity. The crystallographic data showed that the C-B bonds of the central ring are identical ≈ 1.55-1.56 Å for all the phosphorus based structures **65**, **66** and **67**. The C-B bonds (1.52 Å) of **60** are shorter than the equivalent bonds in **65**, **66** and **67** indicating greater electronic delocalisation.

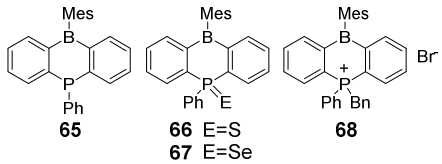

The photophysical properties indicated that all the phosphorus-HBA compounds are blue-shifted compared to the analogous Nitrogen-HBA e.g., for **60** (λ_{max}(abs) = 385 and 404 nm). The photophysical data of the oxidised phosphorus DBHs showed that compound **66** (λ_{max}(abs)=353 and 360nm) is blue-shifted relative to **67** (λ_{max}(abs)=369 and 391nm). The shorter wavelength absorption of phosphonium salt **68** (λ_{max}(abs) = 307, 312 and 381 nm) was assigned to a π-π* transition in the dibenzoheteroborin moiety. Compound **60** exhibited fluorescence in cyclohexane, with a small Stokes shift (λ_{max}(em)= 421 nm, Δλ=17 nm, ϕ= 0.48). The observed blue-shifted compared to **57(N)** was attributed to the smaller π-system. All the P-HBAs are weakly fluorescent and possessed larger Stokes shifts than their nitrogen analogues. The calculated LUMO level (at the B3LYP/6-31G (d) level) for all HBAs, was computed to be

localised on the p_π orbital of the boron atom. The HOMO of **66** and **67** was calculated to reside on sulphur and selenium, respectively, as a predominantly lone pair orbital. The relative Lewis acidity of these compounds was probed by complexation studies with fluoride and chloride. The equilibrium constants of complex formation obtained by titration with the fluoride are: **60** (K=14(3) M^{-1}) < **65** (K=2.1(3)10^4 M^{-1}) < **66** (K=1.4(2)10^5 M^{-1}) < **67** (K=3.3(7)10^6 M^{-1}) < **68** (too large). The complexation of chloride is observed only for three of the series, **66** (K=11(1) M^{-1}) < **67** (K=14(3) M^{-1}) < **68** (K=1.7(1)$10^4 M^{-1}$).

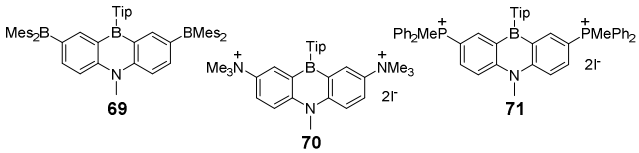

Compound **69** is an analogue of **60** functionalised with $B(Mes)_2$ groups in place of methyls.[70] By introducing two acceptor $B(Mes)_2$ moieties the Lewis acidity of the molecule increased as expected and the photophysical properties were also modified due to a change in the degree of donor-acceptor interactions. The absorption and the fluorescence of **69** (λ_{max}(abs)= 377 nm / (λ_{max}(em)= 402 nm, ϕ= 0.21) were both blue-shifted compared to **60**. Calculations revealed that the LUMO in **69** is predominantly located on the vacant p orbitals of the $B(Mes)_2$ groups and not the endocyclic boron centre, contrary to other HBAs where the LUMO was computed to be localised on the endocyclic boron centre. A fluoride titration study using TBAF in THF was followed by ^{11}B NMR spectroscopy. The resonance at 58 ppm was attributed to the central B of the HBA and that at 72 ppm to the $B(Mes)_2$ groups. During titration, the resonance at 58 ppm persisted but that at 72 ppm disappeared to be replaced by a peak at 5 ppm, in the region of a four coordinate boron atom, corresponding to the formation of a di(fluoroborate) dianion. The UV/vis spectra from titration of F^- (TBAF in THF) showed one isosbestic point after the introduction of one equivalent of fluoride anion and a second after an excess of F^- was added. This demonstrated that the complexation process occurs in two steps with K_1> 10^8 M^{-1} and K_2= 7(1)10^5 M^{-1}, which is larger than that observed for **60** (K= 14(3) M^{-1}).

The further modification of framework **60** by the introduction of other acceptor groups was explored by incorporating cationic ammonio- or phosphonio- groups onto the HBA core (**70** and **71**, respectively).[71] The photophysical data revealed a hypsochromic effect for **70** (λ_{max}(abs)= 393 nm / λ_{max}(em)= 418 nm, ϕ=0.10 in CH_2Cl_2) and **71** (λ_{max}(abs)= 383 nm / λ_{max}(em) =407 nm, ϕ=0.073 in CH_2Cl_2) relative to **60**. Compound **71** was blue-shifted compare to **70** and this was attributed to the stronger electron-withdrawing ability of the cationic phosphonio group. The optical properties were also measured in water, with the maxima of absorption or fluorescence almost identical to those recorded in CH_2Cl_2 ($\Delta\lambda$ < 2nm). In contrast, the quantum yield was found to be much higher in H_2O than in CH_2Cl_2: **70** ϕ= 0.71 and **71** ϕ= 0.48 in H_2O. Highly polar solvents, such as water, generally quench the luminescence through excited-state energy transfer. However, the fluorescence in water is enhanced for these dicationic HBAs a phenomenon attributed to weak interactions between solvent and excited states of these azaborines. Thus the low polarity of the photoexcited states of these azaborines prevents effective luminescence quenching by H_2O. UV-Vis titrations studies were also performed using F^- and CN^- for **70** and **71**. No complexation was observed for compound **70** further confirming its lower Lewis acidity relative to **71** where complexation was observed. The complex formation equilibrium constants shows that the molecule **71** has a higher affinity for cyanide than fluoride anion: $K(F^-)$=1.9(3) 10^2 M^{-1} and $K(CN^-)$ =1.2(4) 10^5 M^{-1} in H_2O/DMSO medium with TBAF.

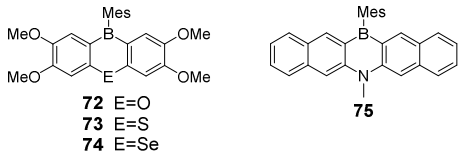

Dibenzoheteroborins have also been reported containing oxygen, sulphur and selenium bridging atoms.[72] The synthesis of the chalcogen HBA analogues utilised the lithiation of bis(2-bromo-4,5-dimethoxyphenyl)-ether, -sulphide or -selenide, followed by the reaction with $MesB(OMe)_2$. The air and moisture stable chalcogen HBAs were obtained in moderate yields (23-39 %). The ^{11}B NMR chemical shifts varied depending on the chalcogen element: O: 52 ppm (**72**); S: 54 ppm (**73**) and Se: 57 ppm (**74**). The shift of the boron resonance up-field was attributed to the increasing strength of the π electronic donation which obviously also impacted the Lewis acidity at boron. The crystallographic data revealed that the HBA core in **72** is planar with the Mes group orientated effectively perpendicular to the HBA plane. The HBA cores in **73** and **74** were slightly twisted with two different angles defined by each terminal phenyl ring deviating from the central heteroborin ring: S : 5.01° and 2.30° ; Se 5.56° and 3.22°. The C-B bond lengths were found to be intermediate between P-HBA and N-HBA congeners. Due to the bulky Mes groups, the π–π interactions between two neighbouring HBA molecules were long for **72** and **73**. However, **74** contains an interaction between the Se atom and the centroid of an adjacent HBA central ring in the extended structure. The optical data showed that these HBAs possess two absorption maxima with the heavier chalcogens being more red-shifted: **72**: λ_{max}(abs)= 320 and 347 nm; **73:** λ_{max}(abs)= 326 and 382 nm; **74**: λ_{max}(abs)= 331 and 392 nm. The shorter absorption wavelengths are attributed to transitions from the HOMO-1, situated on π-orbitals of the benzene rings, to the LUMO. The longer wavelength absorptions were assigned to the HOMO→LUMO transition, an intramolecular charge transfer (ICT) from the lone-pair of oxygen, sulphur or selenium atom to the vacant 2p orbital of the boron centre. Contrary to the absorption data, the fluorescence of these HBAs was found to be solvatochromic. Compound **74** presented a weak fluorescence, but **72** (ϕ=0.30) and **73** (ϕ=0.08) emitted moderately in cyclohexane with a red-shift in dichloromethane. In the solid state, only **72** and **73** displayed significant emission, at 413 and 461nm, respectively. This indicates that the Mes group prevents aggregation in solid state which would otherwise quench the luminescence.

More recently, Kawashima *et al.* developed extended HBAs incorporating a nitrogen atom.[73] The synthesis starts with a

palladium coupling between 2-bromo-3-iodonaphthalene and 3-bromonaphthalen-2-amine. The amino functionality of the intermediate was then methylated with MeI. The last step was lithiation at low temperature (-78°C) followed by addition of $MesB(OMe)_2$. The crystal structure of **75** revealed a slightly bent molecule with a distortion of 15° between the planes of the two naphthyl groups. Short contacts were observed in the solid state with π–π interactions between naphthyl rings and proximate azaborine rings (3.36 Å) and also CH-π interactions between naphthyl rings and the mesityl group. The presence of these interactions was used to explain the quenching of the luminescence of **75** in the solid state. Solution state photophysical studies showed three maxima in the UV/Vis absorption at λ_{max}(abs) = 286, 331 and 519 nm in cyclohexane whereas the diborapentacene analogue **23** presented a single absorption at λ_{max}(abs)= 407 nm. The nitrogen atom has a bathochromic effect again due to the interaction between its lone pair and the formally vacant 2p orbital of the boron atom. Compound **75** emitted at 524 nm, with a small Stokes shift with the emission red-shifted compared to **23** (λ_{max}(em) =410 nm). The electrochemical data revealed a one-electron reversible reduction $E_{1/2}$= -2.1 V (*vs* Fc/Fc^+ in THF), which indicated the formation of a stable radical anion, and a quasi-reversible reduction at E_{pc}= -2.9 V.

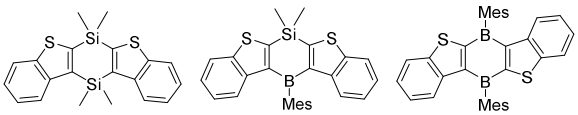

76 **77** **78**

Other HBAs were investigated by Piers and co-workers with the incorporation of a silicon atom into a ladder-type DBH.[74] Three annulated dibenzothiophene compounds were synthesised containing, respectively, Si/Si, Si/B and B/B atoms. The formation of **77** proceeded *via* a mixed Si/Sn compound. The boron centre is protected with a Mes group *via* the introduction of LiMes to the B-halide intermediates. **77** may be converted to **78** although the introduction of the second boron required harsher conditions, specifically heating with BBr_3 at 50°C for 2 days. The B/B molecule was also obtained by the condensation of 2,3-di(dibromoboryl)-benzothiophene, in the same manner to obtain some DBAs (e.g., **23**). Compound **78** adopted an *anti*-conformation, considered as kinetically more stable than the *syn*-conformation. The $NICS(1)_{zz}$ calculations indicated that the central ring in **78**, containing two borons, is antiaromatic in character. The incorporation of a silicon atom into the framework leads to a reduction in antiaromaticity. Calculations (at the B3LYP/6-31G** level) on **76**, **77**, and **78** revealed that for each the HOMO has π character and possesses a node through the centre of the molecule, whereas the LUMO has a contribution from both silicon and boron atoms. A bathochromic effect was observed for each additional boron atom introduced into the skeleton: **76**: λ_{max}(abs)= 307 nm; **77**: λ_{max}(abs)= 379 nm; **78**: λ_{max}(abs)= 427 nm. The optical band gap also followed this trend **76** < **77** < **78**. The emission of **78** revealed a large Stokes shift (λ_{max}(em)= 666 nm, Δλ =230 nm), whereas **76** (λ_{max}(em) =327 nm, Δλ = 20 nm) and **77** (λ_{max}(em) =425nm, Δλ= 46 nm) present a smaller shift. Despite fluorescence investigations, the origin of these differences remained unassigned. Electrochemical studies on these compounds showed that the diborin is the most easily reducible compound relative to the silicon-containing molecules: E_{pc} (**78**) = -0.88 V *vs* Fc/Fc^+ in THF ; E_{pc} (**77**)= -1.66 V.

Summary and Outlook

This review article has summarized the recent progress made in a relatively new and rapidly developing field. Embedding boron into polycyclic aromatics has been demonstrated as an effective method for modulating optoelectronic properties. The incorporated $aryl_3B$ groups function as acceptor moieties reducing the LUMO energy and red shifting absorption / emission bands. Whilst this is attractive for numerous applications simpler synthetic routes are desirable if fused structures with embedded $aryl_3B$ units are to be more widely considered alongside established acceptors (e.g., diketopyrroles, benzothiadiazoles and arylene diimides)[75] in the field of organic optoelectronics. The considerable structural diversity achievable by incorporating $aryl_3B$ moieities, with or without additional heteroatom(s), into fused polycyclics suggests that many more compounds will be accessible *via* currently unexplored synthetic routes. The combined incorporation of B and E (E = NR, S, O etc.) atoms into fused polyaromatics is particularly powerful as it enables controlled modification of both the HOMO and LUMO in these polycyclics. These compounds have potential as ambipolar semiconductors, and whilst only assessed to date in limited cases,[49] good hole and electron mobilities have been predicted for a number of compounds.[76]

Another important potential application of these materials originates in the recent discovery that B and dual B/E doped graphenes are effective catalysts for a number of important reactions, for example as electrocatalysts for the oxygen reduction reaction (ORR)[77] and for the hydrogen evolution reaction.[78] To date synthetic approaches to B / E doped graphenes have been predominantly top down, often *via* conversion of graphene oxide using small molecule boron / E sources.[77] Whilst generating materials with intriguing properties defining structure-property relationships is inherently challenging in these materials due to the heterogeneous nature of the B / E sites (multiple chemical environments are observed by XPS). Nevertheless, multiple studies have indicated excellent electrocatalytic performance in the ORR, particularly for B / N doped graphenes where boron and nitrogen are not directly bonded.[77a] Developing structurally well-defined model complexes of B and B / N doped graphenes and assessing electrocatalytic activity is therefore highly desirable and necessitates the study of structures containing 5, 6 and 7 membered boracycles due to the 5,7-defects that are present in graphene. This is achievable by extending Yamiguchi's pioneering work on the bottom up synthesis of B doped and B / S doped nano-graphenes[41,42,49] or by developing fundamentally new synthetic approaches. It is noteworthy in the context of ORR electrocatalysis to highlight the extremely rapid reaction of *N*-heterocylic carbene stabilized 9-boraanthracenes

Cite this: DOI: 10.1039/c0xx00000x

www.rsc.org/xxxxxx

FEATURE ARTICLE

Table 1: Compilation of the optoelectronic properties of fused structures containing embedded boron atoms in the core.

N°	Solvent[a]	λ_{abs}[nm]	λ_{em}[nm]	ϕ	$E_{1/2}^{red}$ [V][b]	$E_{1/2}^{ox}$ [V][b]	E_{pc} [V][b]	E_{pa} [V][b]
Fused structures containing boroles								
1[9]	THF	361;480	561	0.030	-	-	-	-
1[9]	DMF	372;479	423	0.89	-	-	-	-
1-F[9]	THF	374	419	0.92	-	-	-	-
2[9]	THF	394;488	550	0.041	-	-	-	-
2[9]	DMF	389	419	0.88	-	-	-	-
2-F[9]	THF	400	417	0.86	-	-	-	-
3[9]	THF	405;504	576	0.022	-	-	-	-
3[9]	DMF	425;498	478	0.55	-	-	-	-
3-F[9]	THF	428	478	0.42	-	-	-	-
4[10]	THF	388;470	608	0.24	-2.04; -2.70	-	-	-
4[10]	DMF	390;470	622	0.23	-	-	-	-
5[10]	THF	366;457	600	0.48	-2.19	+0.29;+0.51	-3.0	-
5[10]	DMF	368;460	634	0.25	-	-	-	-
6[11]	CH_2Cl_2	552	-	-	-1.98	-	-2.79	-
7[11]	CH_2Cl_2	469	-	-	-1.96	-	-2.89	-
8[11]	CH_2Cl_2	600	-	-	-1.72	-	-2.61	-
$\mathbf{9}_{TIP}$[11]	THF	410	514	0.09	-2.11	-	-3.05	-
10[14]	CH_2Cl_2	479	-	-	-2.25	+0.62	-3.04	+0.62
11[14]	CH_2Cl_2	468	-	-	-1.97	+0.76	-2.85	+0.76
12[14]	CH_2Cl_2	474	-	-	-1.89	+0.95	-2.78	+0.95
13-Me[17]	C_6H_{12}	430	529	0.21	-	-	-	-
13-Ph[17]	C_6H_{12}	430	527	0.36	-	-	-	-
14-Me[17]	C_6H_{12}	451	537; 567	0.13	-	-	-	-
15[18]	C_6H_{12}	380	519	0.55	-	-	-	-
16[18]	C_6H_{12}	411	513	0.42	-	-	-	-
17[19,20]	CH_2Cl_2	263; 314; 459	-	-	-	-	-2.47;-2.89	-
Diboraanthracenes and other diboraacenes								
21[32]	THF	349; 400	483	0.05	-1.82; -2.78	-	-	-
21[32]	C_6H_{12}	349	413	0.02	-	-	-	-
22[37]	C_6H_6	349	460	0.03	-	-	-	-
22[37]	THF	349	485	0.04	-1.84; -2.73	-	-	-
23[33]	C_6H_{12}	407	410	-	-1.23[c]	-	-	-
24a[36]	C_6H_6	306; 340; 396	490	0.45[)	-1.71	-	-2.48[d]	-
24b[36]	C_6H_6	306; 340; 396	490	0.45	-1.71	-	-2.48[d]	-
24c[36]	C_6H_6	319; 366; 406	469; 494	0.66	-1.83	-	-2.63[d]	-
24d[36]	C_6H_6	332; 388	540	0.25	-1.59	-	-2.39[d]	-
24e[36]	C_6H_6	316; 372	515	0.72	-1.79	-	-2.84[d]	-
24f[36]	C_6H_6	316; 370	524	0.70	-1.62; -2.41[d]	-	-3.16[d]	-
25a[36]	C_6H_6	336; 458	563	0.69	-2.11	-	-	+0.10; +0.38
25b[36]	C_6H_6	336; 458	563	0.69	-2.11	-	-	+0.10; +0.38
25c[36]	C_6H_6	308; 340; 459	594	0.60	-1.86	-	-	+0.30; +0.60
26[37]	C_6H_{12}	355; 416	456	0.04	-	-	-	-
26[37]	C_6H_6	357;422	513	0.04	-	-	-	-
26[37]	THF	355; 416	546	0.09	-1.72; -2.58	-	-	-
26[37]	CH_2Cl_2	354; 418	553	0.12	-	-	-	-
27[37]	C_6H_{12}	373; 519	575	0.10	-	-	-	-
27[37]	C_6H_6	374;531	635	0.05	-	-	-	-
27[37]	THF	374; 523	684	0.03	-1.68; -2.46	-	-3.32	-
27[37]	CH_2Cl_2	374; 524	740	0.01	-	-	-	-
28[37]	C_6H_6	346; 442; 536	644	0.06	-1.70; -2.37; -2.64	-	-3.11	-
29[37]	C_6H_6	359; 429; 556	675	-	-1.69; -2.42	-	-3.27;-3.39	-
30[39]	C_6H_{12}	371; 567	-	-	-1.77; -2.60	-	-3.30	+0.23
31[39]	C_6H_{12}	373; 557	582	0.11	-1.69;-2.50	-	-3.10;-3.40	-
31[39]	CH_2Cl_2	376; 521	700	0.03				
32[40]	toluene	409; 522	632	0.06	-1.68; -2.48	+0.61[d]	-	-
33[40]	toluene	432	447	0.03	-	+0.70; +0.79	-2.23; -2.43; -2.64	-

Fully Fused (di)boraanthracenes								
35[41]	toluene	487; 564; 640	679	0.04	-1.45; -1.66	+0.62	-	-
36[42]	THF	289; 310; 320	407	0.10	-2.59	-	-2.69	-
37[42]	THF	377	384;400	0.10	-2.04; -2.56	-	-2.09;-2.61	-
38.K[47]	THF	375; 412; 500; 531; 568	584; 591; 634	0.45	-	-	-	-
40[48]	THF	391	441	0.92	-2.27; -2.35	+0.90[(e)]	-	-
41[48]	THF	418	482	0.25	-2.27	+0.67[(e)]	-	-
42[49]	toluene	527; 563; 620; 668	729	0.016	-1.37	+0.60	-	-
43[50]	toluene	429; 546	573	0.15	-1.48	-	-	-
Fused structures containing borepins								
44[55]	CH_2Cl_2	260	400	0.70	-	-	-2.56[(d)]	-
45[55]	CH_2Cl_2	280	445	0.39	-	-	-2.25[(d)]	-
46[55]	CH_2Cl_2	314	477	0.01	-	-	-2.20[(d)]	-
51[59]	$CHCl_3$	379	404	0.58	-1.97; -2.20	-	-	-
52a[59]	$CHCl_3$	382	396	0.23	-2.24	-	-	-
52b[59]	$CHCl_3$	380	395	0.38	-2.23	-	-	-
53 (H)[61]	$CHCl_3$	439	456	0.71	-1.89; -2.46	-	-	-
53a[61]	$CHCl_3$	286; 351; 392; 420	460	0.36	-1.99; -2.52	-	-	-
53b[61]	$CHCl_3$	321; 340; 371; 392; 422	465	0.69	-1.93; -2.49	-	-	-
53c[61]	$CHCl_3$	299; 375; 392	463	0.52	-1.85; -2.62	-	-	-
53d[61]	$CHCl_3$	288; 354; 392; 421	465	0.45	-1.89; -2.38	-	-	-
53e[61]	$CHCl_3$	320; 340; 371; 392	464	0.29	-1.84; -2.34	-	-	-
53f[61]	$CHCl_3$	326; 349; 372; 394; 421	465	0.49	-1.83; -2.22	-	-	-
54[62]	$CHCl_3$	407	413	0.80	-2.12	-	-	-
54a[62]	$CHCl_3$	411	441	0.39	-	-	-	-
54b[62]	$CHCl_3$	400	477	0.48	-	-	-	-
55(H)[63]	$CHCl_3$	254; 266; 344; 363	376; 392; 411	0.06	-2.26	-	-	-
56(H)[63]	$CHCl_3$	289; 323; 349; 365	378	0.05	-2.42	-	-	-
55a[63]	$CHCl_3$	265; 297; 440	578	0.08	-1.89	-	-2.35	-
56a[63]	$CHCl_3$	300; 312; 328; 428	493	0.33	-2.01	-	-2.55	-
55b[63]	$CHCl_3$	275; 392; 409; 439	460	0.04	-1.64; -1.94; -2.20; -2.66	-	-	-
56b[63]	$CHCl_3$	296; 309; 328; 361	431	0.02	-1.73; 2.08; -2.58; -3.00	-	-	-
Fused structures containing heteroborins								
57(N)[65]	C_6H_{12}	321; 490; 523	534	0.69	-	-	-	-
57(S)[67]	C_6H_{12}	499	517	0.72	-	-	-	-
58[66]	C_6H_{12}	272; 323; 389; 415	428	0.21	-	-	-	-
59[65]	C_6H_{12}	318; 438; 565; 608	625	0.55	-	-	-	-
60[65]	C_6H_{12}	258; 386; 405	421	0.48	-	-	-	-
60[66]	CH_2Cl_2	385;404	-	-	-	-	-	-
61[66]	C_6H_{12}	580	603	0.12	-	-	-	-
62[66]	C_6H_{12}	568	592	0.20	-	-	-	-
63[66]	C_6H_{12}	529	546	0.98	-	-	-	-
64(N)[66]	C_6H_{12}	609	626	0.55	-	-	-	-
64(S)[67]	C_6H_{12}	558	580	0.61	-	-	-	-
69[70]	C_6H_{12}	377	402	0.21	-	-	-	-
70[70,71]	CH_2Cl_2	393	418	0.10	-	-	-	-
70[70,71]	H_2O	395	420	0.71	-	-	-	-
71[70,71]	CH_2Cl_2	383	407	0.073	-	-	-	-
71[70,71]	H_2O	383	409	0.48	-	-	-	-
72[72]	C_6H_{12}	320; 347	377	0.30	-	-	-	-
73[72]	C_6H_{12}	326; 382	412	0.08	-	-	-	-
74[72]	C_6H_{12}	331; 392	427	0.001	-	-	-	-
75[73]	C_6H_{12}	286; 331; 519	524	0.29	-2.1	-	-2.9[(d)]	-
77[74]	CH_2Cl_2	234; 270; 311; 379	425	0.01	-1.62[(f)]	-	-1.66;-2.50;-2.72[(f)]	-1.59; +0.86[f]
78[74]	CH_2Cl_2	281; 293; 356; 427	666	0.15	-0.82	-	-0.88;-1.63;-1.87	-0.77; +0.96

a) solvent used for photophysical measurements; b) electrochemistry performed in THF versus Fc/Fc^+ unless otherwise stated; c) electrochemistry performed in CH_3CN; d) quasi reversible redox value; e) electrochemistry in CH_2Cl_2; f) electrochemistry in DMF

with O_2 which occurs without a photosensitizer (Scheme 9).[79]

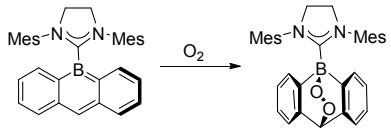

Scheme 9

In contrast related anthracene derivatives require a photosensitizer and the reaction with O_2 take hours not minutes, clearly emphasising the dramatic effect that boron 'doping' can have on the reactivity of polycyclics towards O_2 in a well-defined small molecule. The potential to develop $aryl_3B$ embedded polycyclics further for a range of goals is clear to see, and it is likely that more exciting advances will be made in the near future.

†Notes and references

[a] *School of Chemistry, The University of Manchester, Oxford Road, Manchester, U.K. E-mail: Michael.Ingleson@manchester.ac.uk,*

1. (a) J. Mei, Y. Diao, A. L. Appleton, L. Fang, Z. Bao, *J. Am. Chem. Soc.,* 2013, **135**, 6724; (b) P. M. Beaujuge, J. M. J. Frechet, *J. Am. Chem. Soc.,* 2011, **133**, 20009; (c) C. Wang, H. Dong, W. Hu, Y. Liu, D. Zhu, *Chem. Rev.,* 2012, **112**, 2208.
2. F. Jäkle, *Chem. Rev.,* 2010, **110**, 3985.
3. D. Frath, J. Massue, G. Ulrich, R. Ziessel, *Angew. Chem. Int. Ed.*, 2014, **53**, 2290
4. Comparison of B-N or B-O containing polyaromatic hydrocarbons with B containing polyaromatic hydrocarbons reveal that the latter generally have less negative reduction potentials and red shifted absorbance.
5. (a) Z. Q. Liu, T. B. Marder, *Angew. Chem. Int. Ed*., 2008, **47**, 242; (b) M. J. D. Bosdet, W. E. Piers, *Can. J. Chem*., 2009, **87**, 8; (c) P. G. Campbell, A. J. V. Marwitz, S. Y. Liu, *Angew Chem. Int. Ed.,* 2012, **51**, 6074; (d) E. R. Abbey, A. N. Lamm, A. W. Baggett, L. N. Zakharov, S.-Y. Liu, *J. Am. Chem. Soc*., 2013, **135**, 12908; (e) X.-Y. Wang, J.-Y. Wang, J. Pei, DOI: 10.1002/chem.201405627
6. J. J. Eisch , N. K. Hota , S. Kozima , *J. Am. Chem. Soc.,* 1969, **91**, 4575.
7. A. Steffen, R. M. Ward, W. D. Jones, T. B. Marder, *Coordination Chemistry Reviews*, 2010, **254**, 1950.
8. a) H. Braunschweig, T. Kupfer, *Chem. Commun*., 2011, **47**, 10903; b) H. Braunschweig, I. Krummenacher, J. Wahler, *Advances in Organometallic Chemistry*, 2013, **61**, 1.
9. S. Yamaguchi, T. Shirasaka, S. Akiyama, K. Tamao, *J. Am. Chem. Soc*., 2002, **124**, 8816.
10. A. Wakamiya, K. Mishima, K. Ekawa, S. Yamaguchi, *Chem. Commun.*, 2008, 579.
11. A. Iida, S. Yamaguchi, *J. Am. Chem. Soc.,* 2011, **133**, 6952.
12. A. D. Allen, T. T. Tidwell, *Chem. Rev.*, 2001, **101**, 1333.
13. S. Yamaguchi, T. Shirasaka, S. Akiyama, K. Tamao, *J. Am. Chem. Soc*., 2002, **124**, 8816.
14. A. Iida, A. Sekioka, S. Yamaguchi, *Chem. Sci.*, 2012, **3**, 1461.
15. the nucleus-independent chemical shift (NICS) values by DFT calculations at the B3LYP/6-311+G** level of theory using the geometries derived from the crystal structures
16. The Gutmann Beckett method, measures the chemical shift change ($\Delta\delta$) of $Et_3P{=}O$ in the ^{31}P NMR spectra upon coordination to the boroles see: M. A. Beckett, D. S. Brassington, S. J. Coles, M. B. Hursthouse, *Inorg. Chem. Commun.,* 2000, **3**, 530.
17. D.-M. Chen, Q. Qin, Z.-B. Sun, Q. Peng, C.-H. Zhao, *Chem. Commun*., 2014, **50**, 782.
18. D.-M. Chen, S. Wang, H.-X. Li, X.-Z. Zhu, C.-H Zhao, *Inorg. Chem.,* 2014, **53**, 12532.
19. J. F. Araneda, B. Neue, W. E. Piers, M. Parvez, *Angew. Chem. Int. Ed*., 2012, **51**, 8546.
20. J. Araneda, W. E. Piers, M. J. Sgro, M. Parvez, *Chem. Sci.,* 2014, **5**, 3189.
21. T. B. Tai, V. T. T. Huong, M. T. Nguyen, *Chem. Commun.,* 2014, **49**, 11548.
22. C. Hoffend, F. Schödel, M. Bolte, H.-W. Lerner, M. Wagner, *Chem. Eur. J.*, 2012, **18**, 15394.
23. R. Clément, *Compt. Rend. Acad. Sci. Paris*, 1965, **261**, 4436.
24. D. Kaufmann, *Chem. Ber*., 1987, **120**, 901.
25. J. J. Eisch, B. W. Kotowicz, *Eur. J. Inorg. Chem.*, 1998, **6**, 761.
26. a) W. Schacht, D. Kaufmann, *J. Organomet. Chem.*, 1987, **331**, 139; b) C. Reus, S. Weidlich, M. Bolte, H.-W. Lerner, M. Wagner, *J. Am. Chem. Soc*., 2013, **135**, 12892.
27. M. V. Metz, D. J. Schwartz, C. L. Stern, T. J. Marks, *Organometallics*, 2002**, 21**, 4159.
28. A. Lorbach, A. Hübner, M. Wagner, *Dalton Trans.*, 2012, **41**, 6048.
29. a) A. Lorbach, M. Bolte, H. Li, H.-W. Lerner, M. C. Holthausen, F. Jäkle, M. Wagner, *Angew. Chem. Int. Ed.,* 2009, **48**, 4584; b) A. Lorbach, M. Bolte, H.-W. Lerner, M. Wagner, *Chem. Commun.*, 2010, **46**, 3592.
30. E. Januszewski, A. Lorbach, R. Grewal, M. Bolte, J. W. Bats, H.-W. Lerner, M. Wagner, *Chem. Eur. J.*, 2011, **17**, 12696.
31. A. Hübner, M. Diefenbach, M. Bolte, H.-W. Lerner, M. C. Holthausen, M. Wagner, *Angew. Chem. Int. Ed.,* 2012, **51**, 12514.
32. T. Agou, M. Sekine,T. Kawashima, *Tet. Lett.*, 2010, **51**,5013.
33. J. Chen, J. W. Kampf, A. J. Ashe III, *Organometallics*, 2008, **27**, 3639.
34. J. Chen, Z. Bajko, J. W. Kampf, A. J. III Ashe, *Organometallics*, 2007, **26**, 1563.
35. Y. Sakamoto, T. Suzuki, M. Kobayashi, Y. Gao, Y. Fukai, Y.Inoue, F. Sato, S. Tokito, *J. Am. Chem. Soc.,*2004, **126**, 8138.
36. C. Reus, S. Weidlich, M. Bolte, H.-W. Lerner, M. Wagner, *J. Am. Chem. Soc.*, 2013, **135**, 12892.
37. C. Hoffend, M. Diefenbach, E. Januszewski, M. Bolte, H.-W. Lerner, M. C. Holthausen, M. Wagner, *Dalton Trans.*, 2013, **42**, 13826.
38. C. Hoffend, F. Schödel, M. Bolte, H.-W. Lerner, M. Wagner, *Chem. Eur. J.,* 2012, **18**, 15394.
39. C. Hoffend, K. Schickedanz, M. Bolte, H.-W. Lerner, M. Wagner, *Tetrahedron*, 2013, **69**, 7073.
40. C. Dou, S. Saito, S. Yamaguchi, *J. Am. Chem. Soc.,* 2013, **135**, 9346.
41. C. Dou, S. Saito, K. Matsuo, I. Hisaki, S. Yamaguchi, *Angew. Chem. Int. Ed.,* 2012, **51**, 12206.
42. Z. Zhou, A. Wakamiya, T. Kushida, S. Yamaguchi, *J. Am. Chem. Soc.*, 2012, **134**, 4529.
43. K. Okada, H. Inokawa, T. Sugawa, M. Oda, *J. Chem. Soc., Chem. Commun.,* 1992, 448.
44. T. Kushida, C. Camacho, A. Shuto, S. Irle, M. Muramatsu, T. Katayama, S. Ito, Y. Nagasawa, H. Miyasaka, E. Sakuda, N. Kitamura, Z. Zhou, A. Wakamiya, S. Yamaguchi, *Chem. Sci.,* 2014, **5**, 1296.
45. C. W. Chiu, Y. Kim, F. P. Gabbaï, *J. Am. Chem. Soc.*, 2009, **131**, 60.
46. T. Kushida, S. Yamaguchi, *Organometallics*, 2013, **32**, 6654.
47. T. Kushida, Z. Zhou, A. Wakamiya, S. Yamaguchi, *Chem. Commun.,* 2012, **48**, 10715.
48. A. Shuto, T. Kushida, T. Fukushima, H. Kaji, S. Yamaguchi, *Org. Lett*., 2013, **15**, 6234.
49. S. Saito, K. Matsuo, S. Yamaguchi, *J. Am. Chem. Soc.*, 2012, **134**, 9130.
50. K. Matsuo, S. Saito, S. Yamaguchi, *J. Am. Chem. Soc.*, 2014, **136**, 12580.
51. E. E. van Tamelen, G. Brieger, K. G. Untch, *Tett. Let.,* 1960, **8**, 14.
52. S. M. van der Kerk, J. Boersma, G. J. M. van der Kerk, *J. Organometal. Chem*., 1981, **215**, 303.
53. R. L. Disch, M. L. Sabio, J. M. Schulman, *Tet. Lett*., 1983, **24**, 1863.
54. J. J. Eisch, J. E. Galle, *J. Am. Chem. Soc.,* 1975, **97**, 4436.
55. L.G. Mercier, W. E. Piers, M. Parvez, *Angew. Chem. Int. Ed*., 2009, **48**, 6108
56. L. G. Mercier, S. Furukawa, W. E. Piers, A. Wakamiya, S. Yamaguchi, M. Parvez, R.W. Harrington, W. Clegg, *Organometallics,* 2011, **30**, 1719.
57. A. Iida, S. Saito, T. Sasamori, S. Yamaguchi, *Angew. Chem. Int. Ed.*, 2013, **52**, 3760.
58. I., N. Nazarov, I. I. Zaretskaya, *Izv. Akad. Nauk. SSSR, Ser. Khim*, 1941, 211.
59. A. Caruso, Jr., M. A. Siegler, J. D. Tovar, *Angew. Chem. Int. Ed.*, 2010, **49**, 4213.
60. A. Caruso, Jr., J. D. Tovar, *J. Org. Chem*., 2011, **76**, 2227.
61. A. Caruso, Jr., J. D. Tovar, *Org. Lett.,* 2011, **13**, 3106.
62. D. R. Levine, A. Caruso Jr., M. A. Siegler, J. D. Tovar, *Chem. Commun.*, 2012, **48**, 6256.
63. D. R. Levine, M. A. Siegler, J. D. Tovar, *J. Am. Chem. Soc.,* 2014, **136**, 7132.
64. S. Miyasaka, J. Kobayashi, T. Kawashima, *Tetrahedron Lett*., 2009, **50**, 3467.
65. T. Agou, J. Kobayashi, T. Kawashima, *Org. Lett.,* 2006, **8**, 2241.
66. T. Agou, J. Kobayashi, T. Kawashima, *Chem. Commun.,* 2007, 3204.
67. T. Agou, J. Kobayashi, T. Kawashima, *Chem. Eur. J.,* 2007, **13**, 8051.
68. T. Agou, J. Kobayashi, T. Kawashima, *Inorg. Chem*., 2006, **45**, 9137.
69. T. Agou, J. Kobayashi, T. Kawashima, *Org. Lett*., 2005, **7**, 4373.
70. T. Agou, M. Sekine, J. Kobayashi, T. Kawashima, *Chem. Commun*., 2009, 1894.
71. T. Agou, M. Sekine, J. Kobayashi, T. Kawashima, *Chem. Eur. J.,* 2009, **15**, 5056.

72 J. Kobayashi, K. Kato, T. Agou, T. Kawashima, *Chem. Asian J.,* 2009, **4**, 42.
73 T. Agou, H. Arai, T. Kawashima, *Chem. Lett.*, 2010, **39**, 612.
74 L. G. Mercier, W. E. Piers, R. W. Harrington, W. Clegg, *Organometallics,* 2013, **32**, 6820.
75 K. Takimiya, I. Osaka, M. Nakano, *Chem. Mater.,* 2014¸ **26**, 587.
76 T. B. Tai, V. T. T. Huong, M. T. Nguyen, *J. Phys. Chem. C.*, 2013, **117**, 14999.
77 For selected examples see: a) S. Wang, L. Zhang, Z. Xia, A. Roy, D. W. Chang, J. B. Baek, L. Dai, *Angew. Chem. Int. Ed.,* 2012, **51**, 4209. b) Y. Zheng, Y. Jiao, L. Ge, M. Jaroniec, S. Z., Qiao, *Angew. Chem. Int. Ed*., 2013, **52**, 3110. c) S. Wang, E. Iyyamperumal, A. Roy, Y. Xue, D. Yu, L. Dai, *Angew. Chem. Int. Ed.,* 2011, **50**, 11756. d) J. Jin, F. Pan, L. Jiang, X. Fu, A. Liang, Z. Wei, J. Zhang, G. Sun, G. *ACS Nano,* 2014, 8, 3313.
78 B. R. Sathe, X. Zou, T. Asefa, *Catal. Sci. Technol.,* 2014, **4**, 2023.
79 T. K. Wood, W. E. Piers, B. A. Keay, M. Parvez, *Angew. Chem. Int. Ed.,* 2009, **48**, 4009.